Available online at www.sciencedirect.com
ScienceDirect
Virology 371 (2008) 292–308
VIROLOGY
www.elsevier.com/locate/yviro

Translation mechanisms involving long-distance base pairing interactions between the 5′ and 3′ non-translated regions and internal ribosomal entry are conserved for both genomic RNAs of *Blackcurrant reversion nepovirus*

Alexey Karetnikov *, Kirsi Lehto

Laboratory of Plant Physiology and Molecular Biology, University of Turku, FIN-20014 Turku, Finland

Received 2 July 2007; returned to author for revision 2 August 2007; accepted 4 October 2007
Available online 31 October 2007

Abstract

One of the mechanisms of functioning for viral cap-independent translational enhancers (CITEs), located in 3′ non-translated regions (NTRs), is 3′ NTR–5′ leader long-distance base pairing. Previously, we have demonstrated that the RNA2 3′ NTR of *Blackcurrant reversion nepovirus* (BRV) contains a CITE, which must base pair with the 5′ NTR to facilitate translation. Here we compared translation strategies employed by BRV RNA1 and RNA2, by using mutagenesis of the BRV NTRs in firefly luciferase reporter mRNA, in plant protoplasts. Translation mechanisms, based on 3′ CITEs, 5′ NTR–3′ NTR base pairing and poly(A) tail-stimulation, were found conserved between RNA1 and RNA2. The 40S ribosomal subunit entry at the RNA1 leader occurred, at least partly, via an internal ribosomal entry site (IRES). Two RNA1 leader segments complementary to plant 18S rRNA enhanced translation. A model for BRV RNAs translation, involving IRES-dependent 40S subunit recruitment and long-distance 5′ NTR–3′ NTR base pairing, is discussed.

Keywords: Nepovirus; Translation; Translational enhancer; Non-translated region; Long-distance RNA interaction; RNA secondary structure; Internal ribosomal entry site; 18S rRNA

Introduction

Two main mechanisms of eukaryotic translation initiation can be distinguished. First, in cap-dependent ribosomal scanning, observed in the vast majority of cellular mRNAs, the 40S ribosomal subunit (40S), in a complex with eukaryotic translation initiation factors (eIFs), binds immediately downstream from the 5′ cap structure (m7G(5′)ppp(5′)N) and scans the 5′ leader until selection of the correct start codon (Gallie, 2007; Hinnebusch et al., 2007; Pestova et al., 2007). Second, many mRNAs contain internal ribosome entry sites (IRESs) even very distant from the 5′ end, which recruit 40S to the inner regions of the mRNA. Initially, IRESs have been found in animal viruses from the family *Picornaviridae* and in *Hepatitis C virus* (HCV) (reviewed by Doudna and Sarnow, 2007; Fraser and Doudna, 2007; Jang, 2006). Subsequently, IRESs have been discovered in many other animal viruses (reviewed by Baird et al., 2006; Doudna and Sarnow, 2007; Jan, 2006; Mokrejš et al., 2006; Yilmaz et al., 2006), plant viruses (reviewed by Kneller et al., 2006), animal cellular mRNAs (reviewed by Baird et al., 2006; Elroy-Stein and Merrick, 2007; Mokrejš et al., 2006) and at least three plant cellular mRNAs (Dinkova et al., 2005; Dorokhov et al., 2002; Vanderhaeghen et al., 2006). IRESs, as well as other RNA and protein determinants, are known to confer highly efficient expression of viral genomes (Dreher and Miller, 2006; Kneller et al., 2006; Thivierge et al., 2005).

In a cap-dependent scanning pathway, the stimulatory effect of the cap and poly(A) tail on translation is provided through mRNA circularization, according to the closed-loop model of translation initiation (Hentze et al., 2007; Komarova et al., 2006; Svitkin and Sonenberg, 2006). For mRNA circularization, the cap is bound by eIF4E, the poly(A) tail interacts with the poly(A)-binding protein (PABP), and the loop is closed by simultaneous interactions of both eIF4E and PABP with the scaffolding protein eIF4G (Gallie, 2007; Hentze et al., 2007;

* Corresponding author. Fax: +358 2 3335549.
E-mail addresses: alekar@utu.fi (A. Karetnikov), klehto@utu.fi (K. Lehto).

0042-6822/$ - see front matter © 2007 Elsevier Inc. All rights reserved.
doi:10.1016/j.virol.2007.10.003

Hinnebusch et al., 2007; Pestova et al., 2007; Svitkin and Sonenberg, 2006). In turn, 40S is recruited to the mRNA through a chain of interactions 40S-eIF3-eIF4G or, alternatively, 40S-eIF3-eIF1/eIF5-eIF4G (Gallie, 2007; Hinnebusch et al., 2007; Marintchev and Wagner, 2004; Pestova et al., 2007), and finally the correct start codon is selected followed by the 60S ribosomal subunit joining (Algire and Lorsch, 2006; Pestova et al., 2007).

In addition to the cap and poly(A) tail, the 5′ and 3′ non-translated regions (NTRs) of many eukaryotic mRNAs participate in translational regulation through a variety of mechanisms, leading to enhancement or modulation of translation (Doudna and Sarnow, 2007; Elroy-Stein and Merrick, 2007; Hentze et al., 2007). The regulatory role of NTRs in translation is especially important for viral mRNAs lacking either a cap structure or a poly(A) tail or both. Indeed, despite being uncapped and/or non-polyadenylated, such mRNAs are efficiently translated since they are able to form alternative RNA closed-loop structures, often involving NTRs (Dreher and Miller, 2006; Edgil and Harris, 2006; Gallie, 2007; Kneller et al., 2006; Komarova et al., 2006; Miller and White, 2006; Thivierge et al., 2005).

Translation from uncapped/non-polyadenylated RNAs of *Barley yellow dwarf virus* (BYDV) (Guo et al., 2001; Rakotondrafara et al., 2006) and *Tomato bushy stunt virus* (Fabian and White, 2004, 2006) requires direct base pairing between the 5′ NTR and 3′ NTR. Yet, functional cooperation between the 5′ and 3′ NTRs of other uncapped/non-polyadenylated RNAs seems not to involve base pairing, as proposed for *Satellite tobacco necrosis virus* (Gazo et al., 2004; Meulewaeter et al., 1998) and HCV (Bradrick et al., 2006; Song et al., 2006).

Translation of capped/non-polyadenylated RNA of *Dengue virus* is stimulated by independent action of the 5′ and 3′ NTRs under conditions favoring cap-dependent translation but critically depends on cooperative functioning of the NTRs when cap-dependent translation is compromised (Clyde et al., 2006).

For uncapped/polyadenylated RNAs of *Tobacco etch potyvirus* (TEV) (Gallie, 2001; Gallie et al., 1995; Niepel and Gallie, 1999; Ray et al., 2006) and picornaviruses (Bergamini et al., 2000; Svitkin et al., 2001), the closed-loop structure is proposed to be formed through protein-mediated interaction between an IRES in the 5′ NTR and the poly(A) tail. However, picornaviral translation has been recently shown to depend also on the 3′ NTR (Dobrikova et al., 2003, 2006; López de Quinto et al., 2002). Furthermore, a direct base pairing interaction between the 3′ NTR and 5′ IRES of *Foot-and-mouth disease aphtovirus* (FMDV) (*Picornaviridae*) has been implicated in translational stimulation (Serrano et al., 2006).

Blackcurrant reversion virus (BRV) (family *Comoviridae*, genus *Nepovirus*, subgroup *c*) has a genome composed of two positive-sense RNAs, with a poly(A) tail at the 3′ end and, most probably, a small viral protein covalently linked to the genome (VPg) at the 5′ end, instead of a cap (Latvala-Kilby and Lehto, 1999; Lemmetty et al., 1997; Pacot-Hiriart et al., 2001; Susi, 2004). Each of the two RNAs encodes one large polyprotein, proteolytically cleaved by the viral protease into mature proteins. The 5′ NTRs of RNA1 and RNA2 are quite short (66 and 161 nt, respectively), but the 3′ NTRs are very long (1360 and 1363 nt, correspondingly) (Latvala-Kilby and Lehto, 1999; Pacot-Hiriart et al., 2001). The 3′ NTR sequences are very conserved between RNA1 and RNA2 of the sequenced Type isolate and ten field isolates (Lehto et al., 2004). Previously, we have shown that the RNA2 3′ NTR contains a cap-independent translational enhancer (3′ CITE) (region A2) of a novel class, and long-distance RNA–RNA base pairing interaction between the complementary nucleotide stretches of the 3′ NTR (segment 9C3′) and 5′ NTR (segment 9C5′) is necessary for maximal stimulation of translation (Karetnikov et al., 2006). The poly(A) tail of BRV RNA2 has also been demonstrated to substantially enhance translation (Karetnikov et al., 2006). The RNA2 leader has been found to mediate translation through an IRES mechanism, and its multiple regions complementary to plant 18S rRNA contribute to translational stimulation (Karetnikov and Lehto, 2007). Translation of a reporter mRNA 2F2-A_{50}, containing the *Photinus pyralis* (firefly) luciferase (*fluc*) reporter gene, the NTRs of BRV RNA2 and the poly(A) tail, does not require VPg or any other viral proteins (Karetnikov and Lehto, 2007; Karetnikov et al., 2006), in accordance with earlier studies of potyviruses (Basso et al., 1994; Niepel and Gallie, 1999).

In this work, we tested whether the translation mechanisms, based on the 3′ CITE and 5′ NTR–3′ NTR base pairing, would be conserved between the two BRV genomic RNAs (gRNAs). Also, we examined a role of the poly(A) tail of BRV RNA1 in translational regulation and investigated the putative mechanism of 40S entry at the RNA1 leader.

Results

The poly(A) tail of BRV RNA1 is essential for translation

In this study, we used a wild-type *fluc* reporter construct 1F1-A_{50}, containing the intact 5′ NTR and 3′ NTR of BRV RNA1, and the poly$(A)_{50}$ tail (Fig. 1A). To delete the poly(A) tail, the mutant 1F1 was designed. The corresponding RNAs 1F1-A_{50} and 1F1 were electroporated into protoplasts of *Nicotiana benthamiana*, one of the BRV laboratory host species (Lemmetty et al., 1997).

Eliminating the poly(A) tail from the wild-type 1F1-A_{50} construct reduced FLUC expression 5.3-fold (Fig. 1B, mutant 1F1). To distinguish between effects of this deletion on translational efficiency (rate of protein synthesis) and mRNA functional stability, we carried out a time-course analysis of FLUC accumulation for 1F1 and 1F1-A_{50}, a method successfully used in other translation studies (Gallie et al., 1995; Guo et al., 2001; Karetnikov and Lehto, 2007; Karetnikov et al., 2006; Meulewaeter et al., 1998; Rakotondrafara et al., 2006; Shen and Miller, 2007). This analysis showed that the mutant 1F1 had translational efficiency decreased 4.3-fold, compared to the wild type, while mRNA functional stability was much less altered (Fig. 1C). Therefore, the poly(A) tail of BRV RNA1 contributes significantly to translation.

Effect of overlapping deletions of the RNA1 3′ NTR on translation of reporter RNAs

To determine regions of the RNA1 3′ NTR, involved in translational regulation, we created a series of overlapping

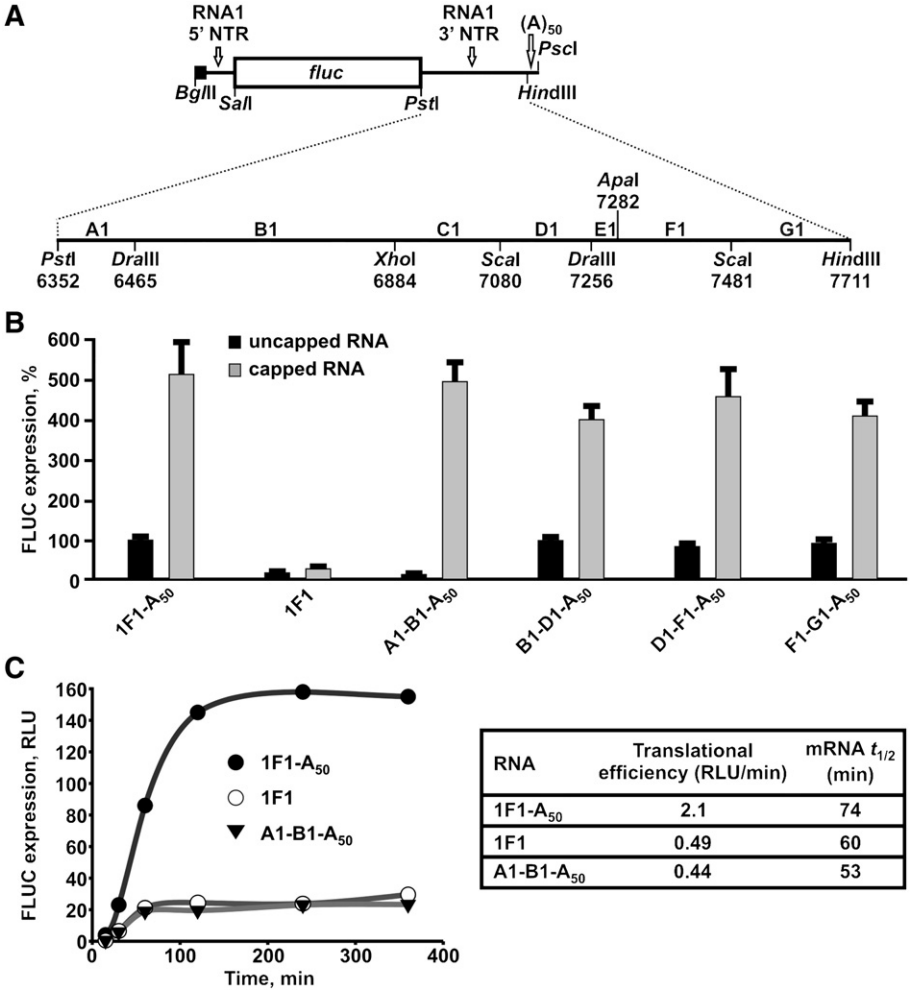

RNA	Translational efficiency (RLU/min)	mRNA $t_{1/2}$ (min)
1F1-A_{50}	2.1	74
1F1	0.49	60
A1-B1-A_{50}	0.44	53

Fig. 1. Effect of the RNA1 3′ NTR and poly(A) tail deletions on FLUC expression in *N. benthamiana* protoplasts. (A) Schematic representation of the 1F1-A_{50} construct and restriction sites used for producing the mutants. A1, B1, C1, D1, E1, F1 and G1 indicate different deleted regions. The T7 promoter is depicted by ■. Numbers correspond to nucleotide positions in RNA1. The RNA elements are indicated by open arrows: open reading frame (box); NTRs (lines); $(A)_{50}$, poly$(A)_{50}$ tail. (B) In vivo FLUC expression from different mutants. FLUC activity was measured following cell lysis 6 h after electroporation with 5 pmol of the indicated transcript, as described in Materials and methods. The mutants are named according to the deleted regions; see panel A. Black columns, uncapped mRNAs; gray columns, capped mRNAs. Columns and bars represent the means + SD, respectively, for three independent experiments, with each protoplast electroporation performed in triplicate. The expression from uncapped 1F1-A_{50} RNA is set at 100%. (C) Time-course analysis of in vivo FLUC expression. The graphs show time-course accumulation of FLUC produced from indicated uncapped RNAs after electroporation into *N. benthamiana* protoplasts. The values for translational efficiencies and mRNA functional half-lives ($t_{1/2}$), determined as described in Materials and methods, are presented on the right. RLU, relative light units.

deletions based on 1F1-A_{50} (Fig. 1A). After RNA electroporation into protoplasts of *N. benthamiana*, the mutants B1-D1-A_{50} (with nt 6466–7256 eliminated), D1-F1-A_{50} (deletion of nt 7081–7481) and F1-G1-A_{50} (nt 7283–7711 deleted) exhibited FLUC production 84–99% of that for the wild type (Fig. 1B). However, removal of the region A1-B1 (nt 6353–6884) resulted in 15% FLUC expression, compared to 1F1-A_{50} (Fig. 1B, mutant A1-B1-A_{50}).

Time-course analysis of FLUC expression, performed for 1F1-A_{50} and A1-B1-A_{50}, revealed that deletion of the stretch A1-B1 affected mostly translational efficiency, diminishing it 4.8-fold, with much less decline in mRNA functional stability (Fig. 1C).

Since the deletions A1-B1 and B1-D1 are overlapping and deletion B1-D1 is almost neutral, these data indicate that the region A1 plays the most important role in translational stimulation by the RNA1 3′ NTR, while the segments B1-G1 provide minor contribution.

The region A1-B1 is a major 3′ determinant of cap-independent translation

To detect elements of the RNA1 3′ NTR, required for cap-independent translation, we tested the effect of adding a 5′-m^{7}G cap to different RNA transcripts on in vivo FLUC expression.

For the wild-type 1F1-A_{50} and mutants B1-D1-A_{50}, D1-F1-A_{50} and F1-G1-A_{50}, the cap stimulated expression 4- to 5.4-fold, when weighed against the corresponding uncapped transcripts (Fig. 1B). Yet, in the case of the deletion mutant A1-B1-A_{50}, the cap enhanced FLUC production 36.1-fold, and the FLUC level not only reached, but even exceeded that of uncapped wild-type 1F1-A_{50} (Fig. 1B). For the mutant 1F1, the

1.5-fold stimulation by the cap was observed (Fig. 1B). Based on these results, we conclude that the region A1-B1 is required for cap-independent expression from the reporter mRNA, and A1-B1 contains a 3′ CITE. However, it should be noted that, although the region A1-B1 is necessary, it may not be sufficient for cap-independent translation.

A combination of the RNA1 NTRs confers efficient translation of a reporter mRNA, while the 3′ CITE functions poorly in the absence of the RNA1 leader

For the uncapped wild-type construct 1F1-A_{50} (with the RNA1 NTRs), FLUC expression in vivo was 91-fold higher than that for uncapped control mRNA CF1-A_{50}, harboring a vector-derived 5′ leader in combination with the RNA1 3′ NTR (Figs. 2A, B). Also, the FLUC level for uncapped 1F1-A_{50} was almost the same as that for m^7G-capped CF1-A_{50} (100% and 87%, respectively; Fig. 2B). For both uncapped RNAs, we performed a time-course analysis of FLUC accumulation in protoplasts. This analysis revealed that mRNA CF1-A_{50} had translational efficiency of 2.3% relative to that of the wild type, while the difference in mRNA functional stabilities was quite small between 1F1-A_{50} and CF1-A_{50} (Figs. 2C, D). Consequently, the combination of the RNA1 NTRs can confer efficient in vivo translation from the *fluc* reporter mRNA, compared to the combination control leader/RNA1 3′ NTR. This indicates also that the RNA1 3′ CITE functions poorly in the absence of the RNA1 leader.

Base pairing between the 5′ leader and 3′ NTR of BRV RNA1 is necessary for translational stimulation

Previously, we have predicted a base pairing potential between the 5′ and 3′ NTRs of RNA1 for the BRV Type isolate (Karetnikov et al., 2006). The complementary segment of a 5′ leader (nt 18–25) is located in a predicted 5′ stem–loop (5′ SL), and here it is referred to as 8C5′ (8-nt complementary sequence of the RNA1 5′ NTR) (Fig. 3). A corresponding 3′ complementary stretch (nt 6361–6368) resides in the predicted SL-1, in the region A1 of the RNA1 3′ NTR, and here it is designated as 8C3′ (8-nt complementary sequence of the RNA1 3′ NTR). Both segments are located mostly in loop parts of the 5′ SL and SL-1, respectively (Fig. 3B in Karetnikov et al., 2006; Fig. 3 of this paper).

To study possible significance of the predicted base pairing interactions between the regions 8C5′ and 8C3′ for translational regulation of the reporter *fluc* mRNAs, we created the mutants 8C5′-A_{50} and 8C3′-A_{50} (Fig. 4A). In these mutants, the stretches 8C5′ or 8C3′, respectively, were replaced by the *Cla*I site AUCGAU, destroying a base pairing potential between the complementary segments (see Fig. 4A and Materials and methods). In addition, we designed a double mutant 8C5′/8C3′-A_{50} with the restored base pairing potential (Fig. 4A).

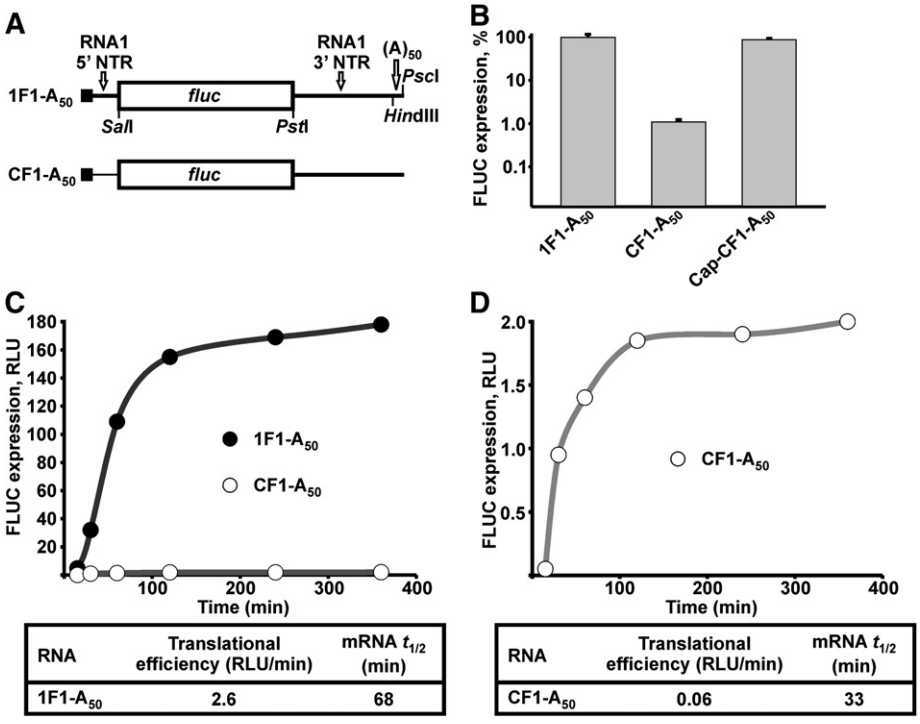

RNA	Translational efficiency (RLU/min)	mRNA $t_{1/2}$ (min)
1F1-A_{50}	2.6	68

RNA	Translational efficiency (RLU/min)	mRNA $t_{1/2}$ (min)
CF1-A_{50}	0.06	33

Fig. 2. A combination of the RNA1 NTRs stimulates efficient FLUC expression in *N. benthamiana* protoplasts. (A) Schematic representation of the *fluc* reporter constructs. Thick lines show viral sequences and thin lines show non-viral sequences. A_{50}, poly(A)$_{50}$ tail. 1F1-A_{50}, wild-type construct; CF1-A_{50}, construct with the control 5′ leader. Other designations are as in Fig. 1A. (B) In vivo FLUC expression from the constructs 1F1-A_{50} and CF1-A_{50}. FLUC activity was measured following cell lysis 6 h after electroporation with 5 pmol of the indicated transcript, as described in Materials and methods. Columns and bars represent the means + SD, respectively, for three independent experiments, with each protoplast electroporation performed in triplicate. The expression from 1F1-A_{50} RNA is set at 100%. (C, D) Time-course analysis of in vivo FLUC expression. The graphs show time-course accumulation of FLUC produced from indicated uncapped RNAs after electroporation into *N. benthamiana* protoplasts. The values for translational efficiencies and mRNA functional half-lives ($t_{1/2}$), determined as described in Materials and methods, are presented below the graphs. RLU, relative light units. The graph in panel D is an extended-scale representation of the plot for CF1-A_{50} from panel C.

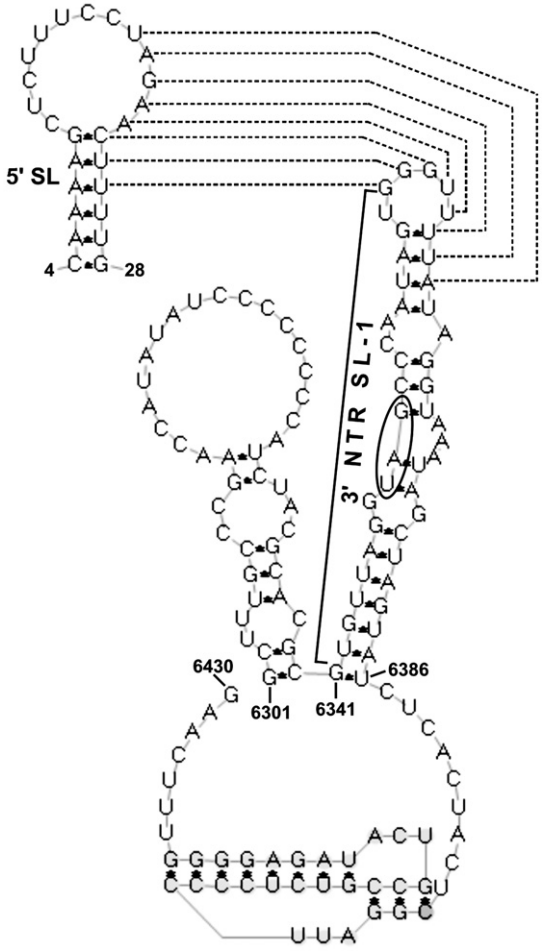

Fig. 3. Schematic representation of the proposed interaction between the 5′ leader and 3′ NTR of BRV RNA1. Base pairing between the 5′ SL and SL-1 is depicted by dashed lines. The 3′ NTR structure includes the 3′ terminal part of the coding sequence of BRV polyprotein 1, but very similar structure was obtained with the FLUC coding region (not shown). The stop codon is circled. Numbers correspond to nucleotide positions in RNA1.

The RNAs of all three mutants and the wild type were electroporated into *N. benthamiana* protoplasts. The constructs 8C5′-A_{50} and 8C3′-A_{50} were characterized by 1.7% and 11% FLUC production of that for the wild type, respectively (Fig. 4B). Nevertheless, the double mutation produced 97% FLUC level, when weighed against 1F1-A_{50} (Fig. 4B).

The addition of a 5′ cap to 1F1-A_{50} and 8C5′/8C3′-A_{50} RNAs enhanced FLUC expression 5.1-fold and 5.3-fold, respectively (Fig. 4B). However, much higher stimulation by the cap was achieved for 8C5′-A_{50} and 8C3′-A_{50} mutants, 45.6-fold and 18.5-fold, correspondingly (Fig. 4B).

According to the data of a time-course analysis of FLUC production, site-directed mutagenesis of the segments 8C5′ and 8C3′ reduced translational efficiency to 3.3% and 20%, respectively, but mRNA functional stability was changed only slightly (Figs. 4C, D). Similarly, the double mutation 8C5′/8C3′ augmented primarily the rate of protein synthesis, which was 4.6-fold higher than that of 8C3′-A_{50} and 27.5-fold higher when weighed against 8C5′-A_{50}, with much less effect on mRNA functional half-life (Figs. 4C, D).

These data suggest that the base pairing interaction between the segment 8C5′ of the RNA1 leader and the stretch 8C3′ of the 3′ NTR is necessary for translational stimulation of the reporter *fluc* mRNA conferred by the RNA1 3′ CITE.

Effect of heterologous combinations of the BRV NTRs on translation

Nucleotide sequences of the BRV 3′ NTRs are very similar between RNA1 and RNA2 — 94.8% identity (Lehto et al., 2004). However, such a resemblance is not observed on the entire length of the 3′ NTRs, and the 5′ proximal part of the RNA1 3′ NTR (nt 6353–6372) does not share similarity with the corresponding region of RNA2 (nt 5043–5065). It is noteworthy that these dissimilar regions represent the 5′ half-stem and loop of the SL-1 elements of both 3′ NTRs, including the RNA2 segment 9C3′, which base pairs with 9C5′ (Karetnikov et al., 2006), and the RNA1 stretch 8C3′, which base pairs with 8C5′ (Fig. 3).

On the other hand, nt 1–40 of RNA1 are identical to nt 2–41 of RNA2, except for three positions (C10, U14 and G28 in RNA1; U11, C15 and C29 in RNA2), and this is the only region of sequence resemblance between the two BRV 5′ leaders (Pacot-Hiriart et al., 2001). This region of high similarity contains the 5′ SL of both RNAs, including the segment 8C5′ (in RNA1) or 9C5′ (in RNA2). Variation in the position C10/U11 makes the predicted secondary structures of the 5′ SL slightly different between the two BRV RNAs due to an enlarged loop in RNA1 (Figs. 4, 6 in Karetnikov et al., 2006; Fig. 3 of this paper).

Thus, in the models of 5′–3′ long-distance base pairing interactions, proposed for RNA2 (Karetnikov et al., 2006) and RNA1 (Fig. 3), the dissimilar 3′ NTR segments 9C3′ and 8C3′, respectively, interact with the stretches 9C5′ and 8C5′, which are located in different but overlapping positions of the almost identical regions of the two BRV 5′ leaders (Fig. 6 in Karetnikov et al., 2006). Consequently, it was interesting to further confirm that the long-distance base pairing mechanism of translation is conserved between the two BRV gRNAs, by placing the RNA2 3′ NTR into the context of the RNA1 leader, and vice versa, using the combination RNA1 3′ NTR/RNA2 leader. Therefore, we designed two reporter *fluc* constructs with both possible heterologous combinations of the BRV NTRs, 1F2-A_{50} (RNA1 leader/RNA2 3′ NTR) and 2F1-A_{50} (RNA2 leader/RNA1 3′ NTR) (Fig. 5A). Two other constructs, 1FC-A_{50} and 2FC-A_{50}, contained a vector-derived control 3′ NTR combined with each of the BRV 5′ leaders (Fig. 5A). The RNA transcripts of these four clones, along with two wild-type constructs, 1F1-A_{50} and 2F2-A_{50}, were electroporated into *N. benthamiana* protoplasts. The RNA 2F2-A_{50} was characterized by FLUC accumulation of 60%, compared to 1F1-A_{50} (Fig. 5B). The combination of the RNA1 leader and RNA2 3′ NTR produced the FLUC amount close to those for 1F1-A_{50} and 2F2-A_{50}, 72% of 1F1-A_{50} (Fig. 5B, construct 1F2-A_{50}). Yet, the expression level for 2F1-A_{50} was only 3.6% relative to 1F1-A_{50}, and it was similar to FLUC production from control RNAs, 1FC-A_{50} and 2FC-A_{50} (Fig. 5B). From these results, we conclude that the RNA1 leader

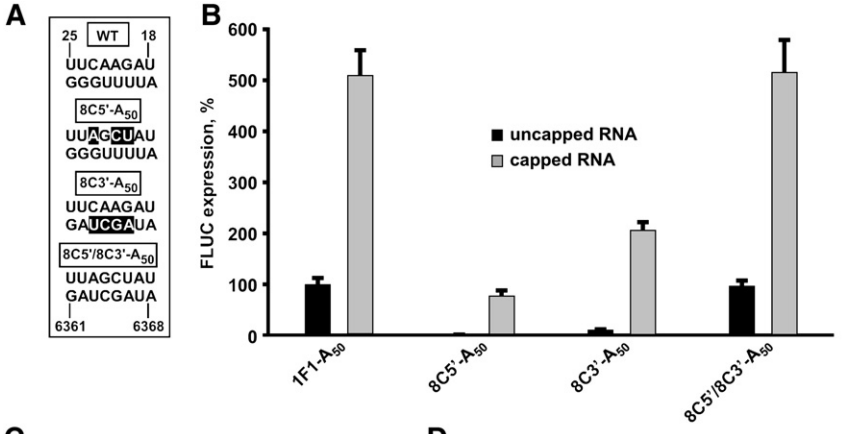

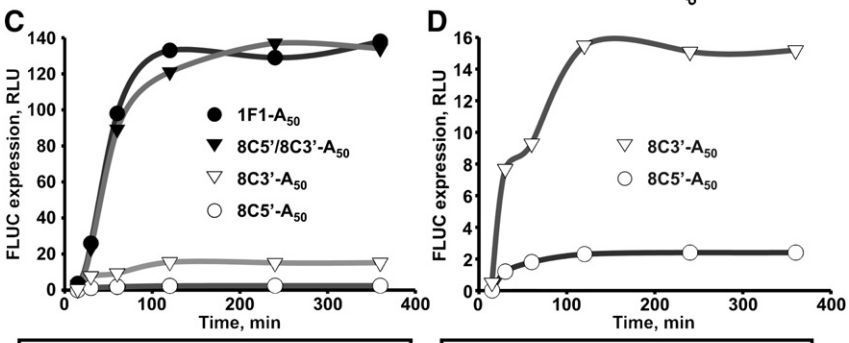

RNA	Translational efficiency (RLU/min)	mRNA $t_{1/2}$ (min)
1F1-A_{50}	2.4	58
8C5'/8C3'-A_{50}	2.2	61

RNA	Translational efficiency (RLU/min)	mRNA $t_{1/2}$ (min)
8C3'-A_{50}	0.48	32
8C5'-A_{50}	0.08	30

Fig. 4. Contribution of base pairing between the NTRs of BRV RNA1 to translation from the *fluc* reporter mRNA. (A) Base pairing potential for the BRV NTRs in the wild-type (WT) and the site-directed mutant *fluc* RNAs. The mutant constructs are named according to mutated sequences, and their names are boxed. White letters on black background show mismatches, introduced by mutations. (B) Effect of the base pairing mutations on FLUC expression in *N. benthamiana* protoplasts. FLUC activity was measured following cell lysis 6 h after electroporation with 5 pmol of the indicated transcript, as described in Materials and methods. Black columns, uncapped mRNAs; gray columns, capped mRNAs. Columns and bars represent the means+SD, respectively, for three independent experiments, with each protoplast electroporation performed in triplicate. The expression from uncapped 1F1-A_{50} RNA is set at 100%. (C, D) Time-course analysis of in vivo FLUC expression from the uncapped base pairing mutants and wild type. The graphs show time-course accumulation of FLUC produced from indicated RNAs after electroporation into *N. benthamiana* protoplasts. The values for translational efficiencies and mRNA functional half-lives ($t_{1/2}$), determined as described in Materials and methods, are presented below the graphs. RLU, relative light units. The graphs in panel D are extended-scale representations of the selected plots from panel C.

is able to confer efficient translation when combined with the RNA2 3′ NTR, while the reverse combination is not effective.

Two regions complementary to plant 18S rRNA stimulate translational efficiency

Unlike the BRV 3′ NTRs, possessing extensive secondary structure (Karetnikov et al., 2004), the 5′ leaders harbor little secondary structure. Thus, the RNA1 leader contains only one predicted relatively stable SL at a 5′ end (5′ SL), which must base pair with the 3′ CITE to facilitate translation (Figs. 3, 6A). To determine whether the RNA1 leader contains translation determinants other than the 5′ SL, we inspected a nucleotide sequence of the leader. This analysis demonstrated that it comprised three 9–13 nt segments, various parts of which were complementary to parts of a region of nt 1113–1121 of plant 18S rRNA, shown previously to be exposed and accessible for intermolecular base pairing and conserved among eukaryotes (Akbergenov et al., 2004). These complementary stretches included 18S-A (nt 10–18), 18S-B (nt 32–44) and 18S-C (nt 46–58) (Fig. 6A). For investigating the putative involvement of these regions in translational regulation, we designed three monocistronic mutants, derivatives of 1F1-A_{50}. In the mutants 18S-B-A_{50} and 18S-C-A_{50}, the longest complementary stretch in either of the two segments 18S-B and 18S-C was subject to site-directed mutagenesis by replacing it with the hexanucleotide AUCGAU (Fig. 6B). The deletion mutant 18S-B/C-A_{50} was devoid of nt 37–58 (stretches 18S-B and 18S-C). After RNA electroporation into *N. benthamiana* protoplasts, the mutants 18S-B-A_{50} and 18S-C-A_{50} exhibited the FLUC levels of 45 and 48%, compared to the wild type (Fig. 6C). The mutant 18S-B/C-A_{50} had FLUC expression reduced to 21% of that of 1F1-A_{50} (Fig. 6C). Time-course expression analysis demonstrated that the observed effects of mutations were primarily due to decrease in rates of protein synthesis (to 30–52% relative to that of the wild type), with mRNA functional half-lives being altered only slightly (to 62–83%) (Fig. 6D). These observations suggest that the regions containing the 18S rRNA-complementary sequences are important for translational stimulation of the monocistronic *fluc* mRNA conferred by the RNA1 5′ NTR.

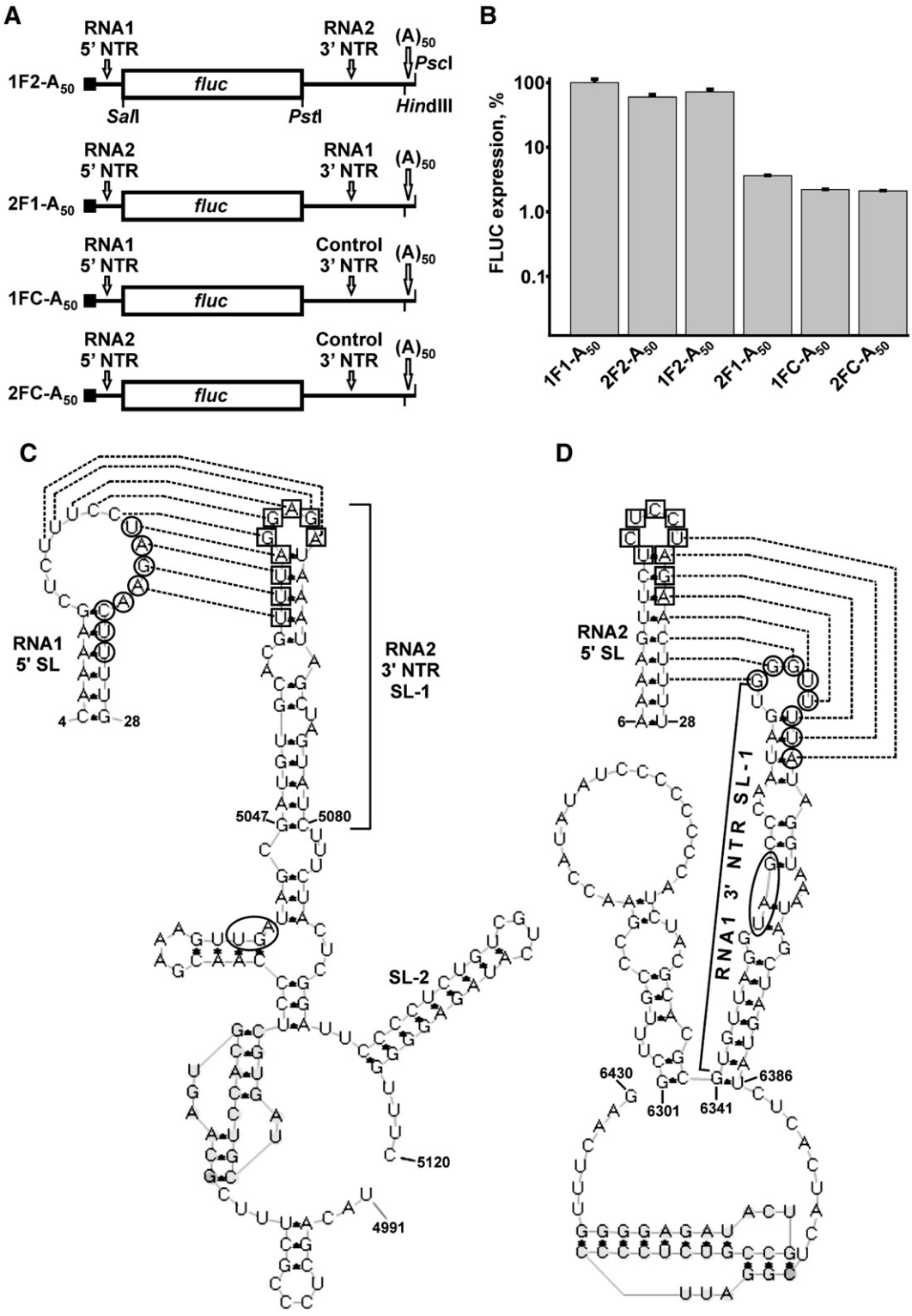

Fig. 5. Effect of homologous and heterologous combinations of the BRV NTRs on FLUC expression in *N. benthamiana* protoplasts. (A) Schematic representation of the constructs with heterologous combinations of the BRV NTRs (1F2-A_{50} and 2F1-A_{50}) and with a control 3′ NTR (1FC-A_{50} and 2FC-A_{50}). The designations are as in Figs. 1A and 2A. (B) In vivo FLUC expression from different uncapped constructs. FLUC activity was measured following cell lysis 6 h after electroporation with 5 pmol of the indicated transcript, as described in Materials and methods. Columns and bars represent the means + SD, respectively, for three independent experiments, with each protoplast electroporation performed in triplicate. The expression from 1F1-A_{50} RNA is set at 100%. (C, D) Schematic representation of putative interactions between the heterologous NTRs of BRV: (C) RNA1 leader and RNA2 3′ NTR; (D) RNA2 leader and RNA1 3′ NTR. Base pairing between the corresponding 5′ SL and SL-1 is depicted by dashed lines. Nucleotides participating in complementary interactions between the RNA2 NTRs (Karetnikov et al., 2006) are boxed, and those involved in base pairing between the RNA1 NTRs are circled. The 3′ NTR structures include the 3′ terminal parts of the coding sequence of BRV polyprotein 2 (C) or polyprotein 1 (D). The stop codons are shown by ovals. Numbers correspond to nucleotide positions in RNA1 and RNA2, as indicated.

Regions complementary to plant 18S rRNA in the RNA1 leaders of other nepoviruses

We have shown elsewhere (Karetnikov and Lehto, 2007) that the RNA2 5′ NTRs of members of the genus *Nepovirus* possess regions complementary to plant 18S rRNA. To analyze whether this would be the case for the RNA1 leaders, we inspected all available nucleotide sequences of RNA1 components of nepoviruses. We found that, in nine of eleven nepoviruses, the RNA1 leaders contained from one up to six 7–11 nt segments complementary to parts of the same region of 18S rRNA, nt 1110–1123 (Table 1). These 18S rRNA-complementary stretches occupied various positions in the 5′ NTRs.

The RNA1 leader harbors the IRES active in vivo

To get insight into the mechanism by which 40S would enter the RNA1 leader, we created a series of dicistronic constructs possessing the *rluc* and *fluc* genes as upstream and downstream cistron, respectively, followed by the RNA1 3′ NTR and poly $(A)_{61}$ tail (Fig. 7). The intergenic region of the construct R1F1-A_{61} was represented by the RNA1 leader, while the corresponding part of the construct RCF1-A_{61} was composed of a vector part and a fragment of the cap-dependent β-globin mRNA leader. As both mRNAs were capped, this approach was aimed to assess the possibility that the FLUC expression would be driven via an IRES mechanism, while the RLUC expression should be conferred through cap-dependent scanning.

Both dicistronic mRNAs were electroporated into *N. benthamiana* protoplasts and the expression ratio of FLUC: RLUC was determined. The construct R1F1-A_{61} had an FLUC: RLUC ratio 8.8-fold higher than that of RCF1-A_{61} (Fig. 7). This difference was a result of very dissimilar FLUC expression levels between the two mRNAs, with the RLUC amount being relatively constant (Fig. 7).

To test whether blocking expression of the upstream cistron would influence translation of the downstream cistron, we introduced a stable SL into the construct R1F1-A_{61} immediately

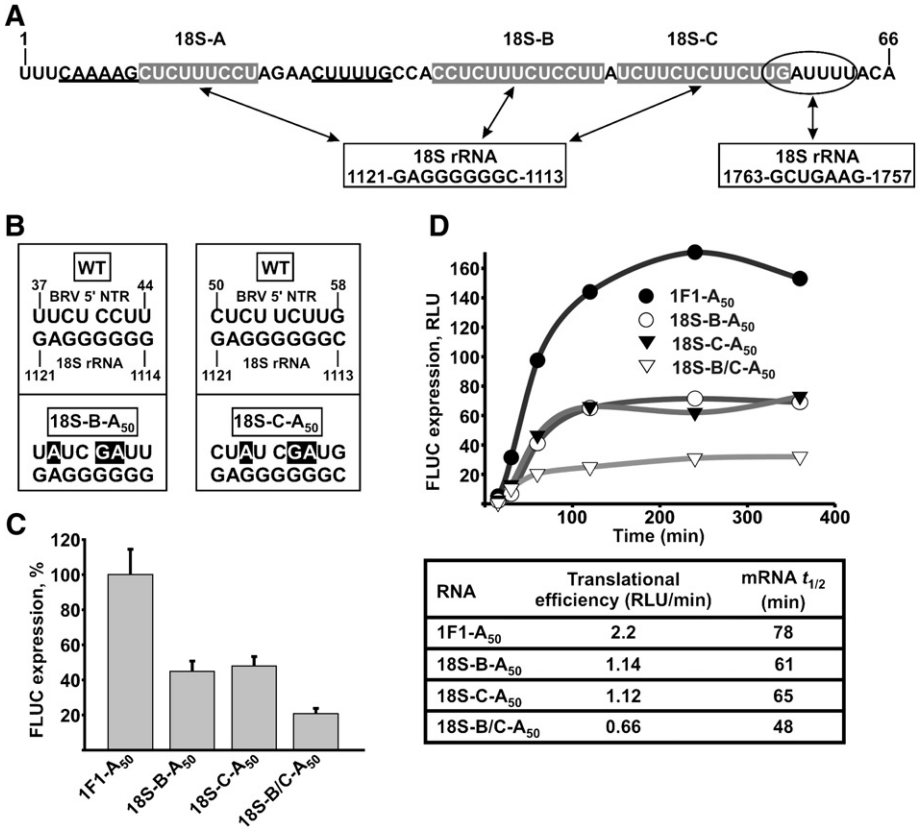

RNA	Translational efficiency (RLU/min)	mRNA $t_{1/2}$ (min)
1F1-A_{50}	2.2	78
18S-B-A_{50}	1.14	61
18S-C-A_{50}	1.12	65
18S-B/C-A_{50}	0.66	48

Fig. 6. Effect of deletion and site-directed mutagenesis of the RNA1 leader regions complementary to nt 1113–1121 of plant 18S rRNA on FLUC expression in *N. benthamiana* protoplasts. (A) Nucleotide sequence of the BRV RNA1 leader. The regions complementary to nt 1113–1121 of plant 18S rRNA (18S-A, 18S-B and 18S-C) are depicted by white letters on a gray background. The region complementary to nt 1757–1763 of plant 18S rRNA is circled. The corresponding 18S rRNA sequences [from Akbergenov et al. (2004), Vanderhaeghen et al. (2006)] are boxed and shown below the BRV sequence. Stem sequences of a 5′ stem–loop are underlined. Numbers correspond to nucleotide positions in RNA1. (B) Potential base pairing between the BRV RNA1 leader and nt 1113–1121 of plant 18S rRNA for the wild-type (WT) and mutant (18S-B-A_{50}, 18S-C-A_{50}) *fluc* RNAs. White letters on a black background show mismatches introduced by the 18S-B and 18S-C mutations. The 18S rRNA sequence is from Akbergenov et al. (2004). (C) In vivo FLUC expression from the wild type and mutant uncapped constructs. FLUC activity was measured following cell lysis 6 h after electroporation with 5 pmol of the indicated transcript, as described in Materials and methods. Columns and bars represent the means+SD for three independent experiments, with each protoplast electroporation performed in triplicate. The expression from 1F1-A_{50} RNA is set at 100%. (D) Time-course analysis of in vivo FLUC expression. The graphs show time-course accumulation of FLUC produced from indicated uncapped RNAs after electroporation into *N. benthamiana* protoplasts. The values for translational efficiencies and mRNA functional half-lives ($t_{1/2}$), determined as described in Materials and methods, are presented below the graphs. RLU, relative light units.

Table 1
Regions complementary to nt 1110–1123 of plant 18S rRNA in the RNA1 leaders of members of the genus *Nepovirus*

Species		RNA sequence/position [a]	
18S rRNA [b]	1123	AUGAGGGGGGCCUU	1110
BRSV	118	….UUU.CUCUUG	126
	151	..AUUU.CUUUUG	160
	190	..GUUC.UUUUC	198
CNSV	10	……..UCUGGGA	16
	71	……..UCUUGGGA	78
GCMV	9	….UUU.UUCC	15
	55	……..U.CUUUUG	61
	64	UACUC.UCCCU	73
	79	……..U.CUUUUG	85
	101	…..UUU.UUUU	107
	164	……..UUUGGGA	170
GFLV	43	…..CUUUUCC.UG	51
	81	……..UCCUU.UG	87
	108	……..CCCCU.CG	114
	169	UACUUU.U	175
PRMV	31	..GCUUU.CUUU	39
	40	UGCUUC.UUUUG	50
RpRSV	47	…..CUCUUCU.CC	55
	60	…..CUCUUCU.U	67
	71	……UCUCUC.U	77
	106	…..UUUUCU.U	112
TBRV	37	...ACUUUCC.CU	45
	79	……..CUCU.UUG	85
	95	UGUUUUC.UUU	104
	105	…..CUCUC.UCU	112
	120	...GCUUUU.CUC	128
ToRSV	27	...ACUUCUC.UC	35
	61	UGUUUUCU.UU	70
	71	……..UCUU.UUG	77
TRSV	38	..ACU.CUCU.UU	46
18S rRNA [b]	1123	AUGAGGGGGGCCUU	1110

Abbreviations: BRSV, *Beet ringspot virus*; CNSV, *Cycas necrotic stunt virus*; GCMV, *Grapevine chrome mosaic virus*; GFLV, *Grapevine fanleaf virus*; PRMV, *Peach rosette mosaic virus*; RpRSV, *Raspberry ringspot virus*; TBRV, *Tomato black ring virus*; ToRSV, *Tomato ringspot virus*; TRSV, *Tobacco ringspot virus*. For the corresponding GenBank accession numbers, see Karetnikov et al. (2006).

[a] Numbers correspond to nucleotide positions in the corresponding RNA.

[b] From Akbergenov et al. (2004).

upstream of the *rluc* gene (Fig. 7, construct SR1F1-A_{61}). The SL insertion diminished the RLUC expression to 1.7% relative to that of R1F1-A_{61}, without significant effect on FLUC level (Fig. 7).

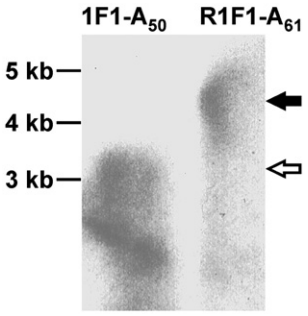

Fig. 8. Northern blot analysis of monocistronic and dicistronic mRNAs with the wild-type BRV RNA1 leader sequence, which resided in the 5′ NTR (1F1-A_{50}) or intercistronic region (R1F1-A_{61}). Total mRNA was extracted from *N. benthamiana* protoplasts 6 h after electroporation with the indicated m^7G-capped transcripts. Northern blotting was carried out by using the digoxigenin-labeled *fluc*-specific RNA probe as described in Materials and methods. The filled arrow shows the position of the full-length R1F1-A_{61} RNA and the open arrow the position of the full-length 1F1-A_{50} RNA. Positions of molecular mass markers are indicated.

To estimate the possibility that FLUC would be expressed from a monocistronic degradation product of R1F1-A_{61} mRNA instead of the full-length dicistronic R1F1-A_{61}, we carried out a Northern blot analysis of total RNA isolated from protoplasts electroporated with either dicistronic R1F1-A_{61} or monocistronic 1F1-A_{50}. For R1F1-A_{61}, we did not observe any outstanding degradation products having a length comparable with that of monocistronic mRNA 1F1-A_{50}, indicating that FLUC was synthesized from the full-length dicistronic R1F1-A_{61} (Fig. 8). These data strongly suggest that expression of the downstream *fluc* cistron stems from the IRES activity of the RNA1 leader rather than from protein synthesis on aberrant mRNAs or termination/reinitiation after translation of the upstream cistron.

Discussion

Translation mechanisms may differ between RNA components of viruses with several (more than one) gRNAs or subgenomic RNAs (sgRNAs). This has been demonstrated, for instance, for uncapped/non-polyadenylated gRNAs of *Red clover necrotic mosaic virus* (family *Tombusviridae*, genus *Dianthovirus*), in which the RNA1 3′ NTR contains a "3′-

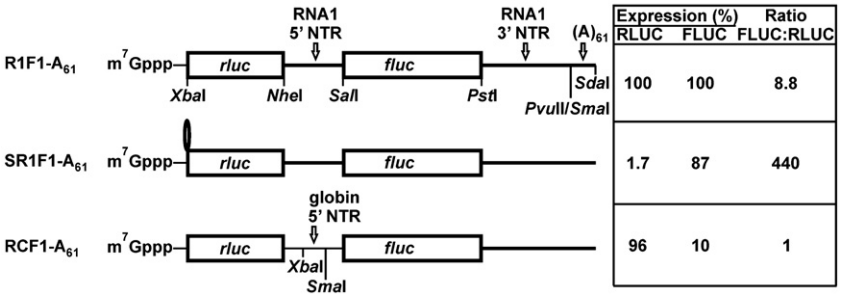

Fig. 7. In vivo FLUC and RLUC expression from dicistronic constructs. The oval indicates a stable stem–loop introduced into SR1F1-A_{61}. Other designations are as described for Figs. 1A and 2A. FLUC and RLUC activities were measured following cell lysis 6 h after electroporation with 5 pmol of the indicated m^7G-capped transcript, as described in Materials and methods. The relative expression values and FLUC:RLUC expression ratios are presented on the right. The expression from R1F1-A_{61} RNA is set at 100%, and the FLUC:RLUC ratio for RCF1-A_{61} is set as 1.

translation element of *Dianthovirus* RNA1" (3′ TE-DR1), required for cap-independent translation (Mizumoto et al., 2003). However, such a 3′ CITE has not been detected in RNA2, which is translated in a cap-independent fashion only in the presence of two RNA1-encoded viral proteins required for replication, p27 and p88, and only when *cis*-acting RNA2 replication elements are intact. This suggests that only RNA2 synthesized de novo is translated (Mizumoto et al., 2006).

In the case of *Tobacco mosaic virus* (TMV) U1, the 75-nt 5′ leader of uncapped/non-polyadenylated sgRNA I_2, comprising the mRNA for movement protein, harbors the IRES (Skulachev et al., 1999). Nonetheless, a coat protein sgRNA is capped and hence uses a cap-dependent translation mechanism (Guilley et al., 1979).

Therefore, it is important to study the translation mechanisms of all gRNAs of viruses with a fragmented genome (or with several sgRNAs). In this work, we compared translation strategies driven by the RNA1 and RNA2 NTRs of BRV, by using the *fluc* and *rluc* reporter constructs. We found that the RNA1 3′ NTR contained the 3′ CITE (Fig. 1), most probably located in its 5′ proximal part (region A1, nt 6353–6465), similarly to the 3′ CITE of BRV RNA2 (region A2) identified earlier (Karetnikov et al., 2006). The region A1-B1 was necessary for efficient cap-independent translation and it could be replaced functionally by a 5′ cap (Fig. 1), like 3′ CITEs of other uncapped viral RNAs (Batten et al., 2006; Danthinne et al., 1993; Koh et al., 2002, 2003; Qu and Morris, 2000; Scheets and Redinbaugh, 2006; Timmer et al., 1993; Wang and Miller, 1995; Wang et al., 1997; Wu and White, 1999).

Another feature, common between translation mechanisms of the two BRV gRNAs, is long-distance RNA–RNA base pairing between a 5′ leader and 3′ NTR. The 8-nt complementary segments of RNA1, 8C5′ (nt 18–25) and 8C3′ (nt 6361–6368), resided in the 5′ SL and SL-1, respectively, and base pairing between them were required for cap-independent translational stimulation of the reporter *fluc* mRNA (Figs. 3, 4). As considered above, the 5′ SLs are almost identical between the two RNAs, differing only by the size of the loop part due to the C10/U11 transition, while the SL-1 elements are very dissimilar between RNA1 and RNA2 (Figs. 4, 6 in Karetnikov et al., 2006; Fig. 3 of this paper). The complementary sequences of the 5′ SLs of RNA1 and RNA2, segments 8C5′ and 9C5′, respectively, represent overlapping parts of the almost identical regions of the two BRV 5′ leaders, and they base pair with mutually unrelated stretches 8C3′ and 9C3′ (Fig. 6 in Karetnikov et al., 2006).

To further corroborate a conserved mechanism of translation between RNA1 and RNA2, we tested the translational activities of heterologous combinations of the BRV NTRs. The RNA1 leader provided efficient translation when combined with the RNA2 3′ NTR, but the RNA2 leader could not function effectively in conjunction with the RNA1 3′ NTR (Fig. 5). In this regard, it is worth mentioning that the high translation level correlated with the availability of a 5′ leader segment for base pairing with the corresponding complementary stretch of a heterologous 3′ NTR (Fig. 5). Indeed, the RNA1 5′ SL sequence, complementary to the RNA2 SL-1, was shifted upstream, compared to 8C5′, and resided entirely in the loop (Fig. 5C). Yet, the RNA2 5′ SL segment, having a potential to base pair with the RNA1 SL-1, was located downstream of 9C5′ and almost completely masked inside the stem part of the RNA2 5′ SL (Fig. 5D). Thus, a predicted RNA2 5′ SL-RNA1 SL-1 base pairing would be expected to be constrained, reflecting the low translation level for the construct 2F1-A_{50} (Figs. 5B, D). The observation that the combination RNA1 leader/RNA2 3′ NTR confers efficient translation, as do both homologous sets of the BRV NTRs, strongly supports a suggestion that the translation mechanism, based on the 5′ NTR–3′ NTR base pairing, is conserved between the two BRV gRNAs. By using a similar approach, though involving various combinations of NTRs of viruses from two different families, it has recently been shown that the translation mechanisms, based on the 5′ NTR–3′ NTR interaction, are conserved (and can be reconstructed) between sgRNA2 of *Tobacco necrosis virus-A* (TNV-A) (genus *Necrovirus*, family *Tombusviridae*) and gRNA of BYDV (genus *Luteovirus*, family *Luteoviridae*) (Meulewaeter et al., 2004), and also between TNV-D and BYDV (Shen and Miller, 2004). As in our experiments, translation levels correlated with changes in the 5′ NTR–3′ NTR base pairing potential depending on the combination of the NTRs used (Meulewaeter et al., 2004; Shen and Miller, 2004).

Similarly to the differential effect of mutations on capped versus uncapped constructs with the RNA2 NTRs (Karetnikov et al., 2006), the A1-B1 deletion and site-directed mutations 8C5′ and 8C3′ caused much stronger decrease in FLUC expression for uncapped transcripts, compared to the capped ones (Figs. 1B, 4B). Likewise, the double mutation 8C5′/8C3′ rescued translation of the single mutants 8C5′-A_{50} and 8C3′-A_{50} considerably more effectively in the case of the uncapped RNAs, when weighed against the capped variants (Fig. 4B). We explain such a distinct influence of mutations on capped versus uncapped RNAs by the existence of functional redundancy in capped/polyadenylated wild-type and 8C5′/8C3′-A_{50} transcripts, which have two ways of mRNA circularization — via the 5′ NTR–3′ NTR kissing SL interactions and the protein-mediated cap-poly(A) mechanism. Capped mutants A1-B1-A_{50}, 8C5′-A_{50} and 8C3′-A_{50} are not able to use the 5′ NTR–3′ NTR base pairing, but preserve the cap-poly(A)-dependent pathway. Uncapped variants of these three mutants have lost a capacity of their mRNAs to be circularized by any of the two mechanisms. These observations provide further evidence that the translation strategies, based on the 5′ NTR–3′ NTR long-distance base pairing, are conserved between BRV RNA1 and RNA2. Similar RNA circularization through 5′ NTR–3′ NTR base pairing has been predicted earlier for both RNA1 and RNA2 of other members of the genus *Nepovirus* (Fig. 5 in Karetnikov et al., 2006).

One more aspect, shared by translation strategies of the two BRV gRNAs, is translational stimulation by the poly(A) tail, a native 3′ element of members of the family *Comoviridae*. In our experiments, the $poly(A)_{50}$ tail enhanced reporter *fluc* mRNA expression 5.3-fold, and this effect was primarily at the level of protein synthesis rate (Fig. 1). This value of stimulation was quantitatively comparable with 4.2-fold enhancement observed previously for the construct with the RNA2 NTRs (Karetnikov

et al., 2006). The poly(A) tail and PABP have been shown to play important roles in translational regulation in many molecular systems (Bergamini et al., 2000; Dobrikova et al., 2006; Gallie et al., 1995; Kahvejian et al., 2005; Svitkin et al., 2001), and our studies of BRV RNA1 and RNA2 demonstrate that the poly(A) tail is essential for translation of even those mRNAs that contain very long (1360 nt) 3′ NTRs harboring CITEs.

We have shown previously that deletion of the C2 region of the RNA2 3′ NTR decreased FLUC expression to 41%, and site-directed mutagenesis of the segment 6C3′, located in the SL-14 of C2 and complementary to the RNA2 5′ SL, resulted in the FLUC level 43% of that for the wild type (Karetnikov et al., 2006). The RNA1 3′ NTR contained a predicted SL (RNA1 SL-14) almost identical to the RNA2 SL-14, and 6 nt (nt 7351–7356) of the RNA1 SL-14 were complementary to the corresponding part (nt 16–21) of the stretch 8C5′ in the RNA1 5′ SL (Karetnikov et al., 2004, 2006). Nevertheless, eliminating the region F1 (nt 7283–7481), harboring the RNA1 SL-14, by deletions D1-F1 and F1-G1 produced the FLUC levels close to that for the wild type (Fig. 1B). Therefore, base pairing between RNA1 nt 16–21 and 7351–7356 is dispensable for translation. The observed difference in functional effects of deleting the SL-14-containing region between the NTRs of RNA1 and RNA2 is not straightforward to interpret. It would be interesting to test whether the full-length RNA2 translation depends on mRNA circularization through alternate use of two pairs of kissing regions, 9C5′/9C3′ and 9C5′/6C3′.

The observed translation enhancement conferred by the RNA1 leader was mediated, at least in part, through the IRES mechanism. The relative translation activity driven by each of the BRV 5′ leaders (relative to the control 5′ NTR) was higher in monocistronic constructs, compared to dicistronic constructs: 91-fold versus 8.8-fold stimulation for the RNA1 leader (this paper) and 333-fold versus 17-fold for the RNA2 leader (Karetnikov and Lehto, 2007). Thus, we cannot exclude a possibility that the IRES mechanism could operate in parallel with 5′ end-dependent/cap-independent scanning on *fluc* reporter mRNAs with the BRV NTRs.

Viral IRESs are very diverse in their location in an mRNA. For instance, in *Dicistroviridae*, IRESs reside in intergenic regions of uncapped dicistronic mRNAs (dicistroviruses also have IRESs in the 5′ leaders) (Doudna and Sarnow, 2007; Jan, 2006). Most of viral IRESs occur in uncapped mRNAs of positive-strand RNA viruses, and the majority of them reside in 5′ NTRs. The uncapped mRNA of giardiavirus (with a double-stranded RNA genome) contains the IRES expanding across both a 5′ leader and an open reading frame (Garlapati and Wang, 2004, 2005). In this study and in the previous work (Karetnikov and Lehto, 2007), we showed that the presence of the 5′ leader sequences was sufficient for the IRES activities, but future experiments would be needed to determine whether the BRV coding regions contribute to the full activities of the BRV IRESs.

The IRES-containing 5′ NTRs of potyviruses *Potato virus Y* (Levis and Astier-Manifacier, 1993), *Turnip mosaic virus* (Basso et al., 1994) and TEV (Gallie, 2001; Niepel and Gallie, 1999; Ray et al., 2006; Zeenko and Gallie, 2005) have a length of only 143–144 nt, and they are moderately structured. Indeed, it has been shown that the TEV IRES contains pseudoknots, important for IRES activity (Zeenko and Gallie, 2005). Nevertheless, the IRES-containing BRV RNA1 leader was much shorter (66 nt) than those of potyviruses and BRV RNA2 (161 nt), and it possessed only one predicted relatively stable SL (5′ SL) (Figs. 3, 6A). The IRES-containing 5′ NTRs of movement protein sgRNAs of crucifer-infecting tobamovirus (crTMV) and TMV U1 are moderately structured but have a length of 75 nt, similar to that of BRV RNA1 leader (Skulachev et al., 1999; Zvereva et al., 2004). Yet, such absence of extensive RNA secondary structure is in common with the IRES-containing 5′ NTRs of *Rhopalosiphum padi virus* (RhPV) from the family *Dicistroviridae* (Terenin et al., 2005) and BRV RNA2 (Karetnikov and Lehto, 2007), both of which are substantially longer than that of BRV RNA1. It should be noted, however, that viral IRESs may be even shorter than those described for BRV RNA1, crTMV and TMV U1. For instance, the IRES of an acyclovir-resistant strain of *Herpes simplex virus* has a length of just 12 nt (Griffiths and Coen, 2005). It is possible that these poorly structured IRESs could effectively recruit eIFs, as proposed for RhPV (Terenin et al., 2005).

We found three stretches in the RNA1 leader, 18S-A (9 nt), 18S-B (13 nt) and 18S-C (13 nt), complementary to nt 1113–1121 of plant 18S rRNA (Fig. 6A). Site-directed mutagenesis of 18S-B or 18S-C, or deletion of both of them, reduced translational efficiency substantially (Fig. 6). The corresponding 18S rRNA sequence is a part of the larger region, nt 1105–1124, shown previously to be conserved among eukaryotes, to be exposed and accessible for intermolecular mRNA-18S rRNA base pairing and to enhance translation when the complementary mRNA part is located in either the 5′ leader or intergenic region of mRNA (Akbergenov et al., 2004). A similar base pairing between the same 18S rRNA region and at least some of the six 8–10 nt stretches (18S1–18S6) of the BRV RNA2 leader has been proposed to contribute to the RNA2 IRES activity (Karetnikov and Lehto, 2007). Unlike the situation observed for RNA2, site-directed mutagenesis of either 18S-B or 18S-C resulted in smaller (decrease to 45–48%; Fig. 6) effect on translation than did the mutagenesis of a single RNA2 region 18S5 (decline to 14%; Karetnikov and Lehto, 2007). However, simultaneous eliminating both 18S-B and 18S-C produced dramatic drop in translation (to 21%; Fig. 6). Such functional redundancy of the 18S rRNA-complementary sequences of the RNA1 leader could be explained by the absence of unpredicted changes in RNA secondary structure in mutants or relatively high independence in functioning each of the two segments, in contrast to the RNA2 leader (Karetnikov and Lehto, 2007). Base pairing interactions between mRNAs and various accessible, conserved 18S rRNA stretches have been proposed to stimulate translation in other eukaryotic systems (Akbergenov et al., 2004; Dresios et al., 2006; Hu et al., 1999; Tranque et al., 1998; Vanderhaeghen et al., 2006; Yang et al., 2003), including viral and non-viral IRES elements, e.g. the TEV IRES (Zeenko and Gallie, 2005). These data appear to be consistent with the "ribosome-filter" (Mauro and Edelman, 2002) and "ribosomal tethering and clustering" hypotheses (Chappell

et al., 2006). According to these theories, direct mRNA-18S rRNA base pairing makes an important contribution to 40S recruitment to many eukaryotic mRNAs, and "tethering" 40S to an IRES or their "clustering" on several neighboring IRES elements (without scanning the mRNA from the 5′ end) facilitates interaction between the methionyl-initiator tRNA anticodon and the initiation codon, which resides at the optimal distance from 40S recruitment site and which is not masked by RNA secondary structure or RNA-binding protein (Chappell et al., 2006; Mauro and Edelman, 2002). It is noteworthy that the "ribosome-filter" and "ribosomal tethering and clustering" hypotheses explain even those cases of translation where IRESs stimulate translation from the upstream start codons (Herbreteau et al., 2005; Jaag et al., 2003; Jünemann et al., 2007; Yilmaz et al., 2006). Recently, direct evidence to support these theories has been provided (Chappell et al., 2006; Dresios et al., 2006), and our results suggest that the 18S rRNA-complementary segments play the important role in functioning of BRV IRESs. Also, sequences complementary to the same 18S rRNA region are present in the RNA1 leaders of other nepoviruses (Table 1).

In addition, we found that the RNA1 5′ NTR contains a segment of nt 57–63 complementary to nt 1757–1763 of plant 18S rRNA (Fig. 6A), located in a single-stranded part of its 3′ end and demonstrated previously to stimulate the IRES activity of plant ribosomal protein S18 mRNA by base pairing with mRNA (Vanderhaeghen et al., 2006).

It is worth mentioning that the segments 18S-A, 18S-B and 18S-C resided in the polypyrimidine-rich tracts (Fig. 6A), important translation determinants of various IRES-containing viral and cellular mRNAs (Florez et al., 2005; Mitchell et al., 2005; Song et al., 2005). Therefore, we cannot exclude the possibility that 18S-B and/or 18S-C might stimulate BRV translation through interactions of the polypyrimidine-rich tracts with a predicted plant polypyrimidine tract-binding protein (Marin and Boronat, 1998).

Based on the results of this study and on our previous results (Karetnikov and Lehto, 2007; Karetnikov et al., 2006), we propose a hypothetical model describing translation mechanisms for both BRV RNAs (Fig. 9). It should be noted that the model represents a working hypothesis for further testing and hence does not pretend to be finalized and comprehensive. According to this model, 40S would be recruited to the 5′ NTR IRES, and after translation termination the 5′ NTR–3′ NTR base pairing might facilitate efficient recycling of ribosomal subunits again to the 5′ end of the mRNA, by holding two mRNA ends in close proximity (Fig. 9). Apart from BRV, long-distance 5′ NTR–3′ NTR base pairing has been suggested recently to facilitate IRES-driven translation in FMDV, which contains uncapped/polyadenylated mRNA, similarly to BRV (Serrano et al., 2006). Both BRV (Fig. 9) and FMDV (López de Quinto et al., 2002; Serrano et al., 2006) are likely to harbor at least two alternative mechanisms of mRNA circularization, first mediated by the 5′ NTR–3′ NTR base pairing and the second one mediated by the poly(A) tail/PABP. Although the role of the poly(A) tail-PABP-eIF4G-IRES interaction in translation of *Picornaviridae* has been well-studied, the interacting 5′ partner of the BRV poly(A) tail/PABP is unknown (Fig. 9). Thus, such long-distance complementary interactions between the 5′ and 3′ NTRs, presenting an alternative mode of mRNA closed-loop formation typical for eukaryotes (Hentze et al., 2007; Komarova et al., 2006; Svitkin and Sonenberg, 2006), are not limited to uncapped/non-polyadenylated mRNAs of *Luteoviridae* and *Tombusviridae*, lacking IRESs (Fabian and White, 2004, 2006; Guo et al., 2001; Rakotondrafara et al., 2006; reviewed by Miller and White, 2006), but occur also in viral mRNAs with different modifications of the ends, including uncapped mRNAs with the poly(A) tails and 5′ NTR IRESs. As a further test for our model of BRV NTRs-driven translation, it would be interesting to see how the simultaneous compromising of all possibilities for mRNA circularization, (i) through 9C5′/9C3′ for RNA2 or 8C5′/8C3′ for RNA1, (ii) through 9C5′/6C3′ for RNA2 and (iii) through the poly(A) tail for both gRNAs, might affect the BRV IRES function in the dicistronic context. This would help to reveal whether the BRV 5′ leaders serve independently on the 5′ NTR–3′ NTR base pairing.

In conclusion, we found that the translation mechanisms, based on 3′ CITEs, long-distance 5′ NTR–3′ NTR base pairing interactions, stimulation by the 3′ poly(A) tail and 40S recruitment to 5′ IRESs, are conserved between the two BRV gRNAs, although some important differences exist between RNA1 and RNA2.

Materials and methods

RNA secondary and tertiary structure predictions

RNA secondary and tertiary structures were predicted by RNA folding simulations, using a genetic algorithm (Gultyaev et al., 1995), implemented in the package STAR (http://wwwbio.leidenuniv.nl/~batenburg/STAR.html), at 25 °C. The structures were visualized using the PseudoViewer2 program (Han and Byun, 2003).

cDNA constructs

Virion BRV RNA was isolated from infected *Chenopodium quinoa* plants, as described previously (Lemmetty et al., 1997). RNA1 cDNA has been produced previously as described by Pacot-Hiriart et al. (2001). The T7 promoter sequence was fused to a 5′ terminal clone to initiate transcription from the first viral nucleotide.

Clones pRL-SV40 and pPVc702, containing *rluc* and *fluc* reporter genes, were a kind gift of Matti Karp and Pekka Virtanen (University of Turku, Finland). To obtain 1F1, the RNA1 5′ NTR was PCR-amplified with primers 1 and 2, the *fluc* gene with primers 3 and 4 and the RNA1 3′ NTR with primers 5 and 6 (Table 2). The corresponding DNA fragments were digested with relevant restriction endonucleases and cloned into pUC19 (Fig. 1A). For designing 1F1-A_{50}, two complementary oligonucleotides, 7 and 8 (Table 2), were introduced into 1F1, using the sites *Hin*dIII and *Psc*I.

To obtain A1-B1-A_{50}, the *Sal*I–*Pst*I *fluc* fragment was inserted into pCR-BluntII-TOPO (Invitrogen), resulting in *fluc*-

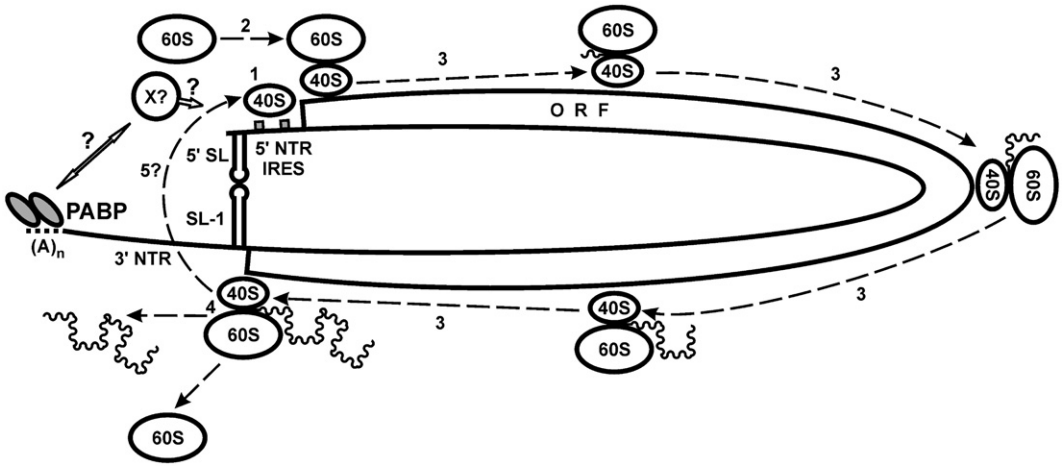

Fig. 9. A hypothetical model (working hypothesis) describing mechanisms of translation for BRV RNAs. 1, the 40S ribosomal subunit (small oval) is recruited to the 5′ NTR IRES, and base pairing between plant 18S rRNA and the corresponding complementary sequences of the BRV 5′ leader (shown as two small gray boxes) may facilitate this process. 2, after the start codon recognition, the 60S ribosomal subunit (large oval) joins to form the 80S initiation complex. 3, during translation elongation, the polyprotein (thin curly line) is synthesized. 4, after translation termination, the 80S complex is disassembled and the polypeptide is released. 5, long-distance RNA–RNA base pairing between the 5′ SL of the BRV 5′ leader and the SL-1 of the 3′ NTR holds two mRNA ends in close proximity, thus facilitating recycling of the ribosomal subunits again to the 5′ NTR. In addition to the 5′ NTR–3′ NTR base pairing, an alternative way of mRNA circularization is supposed to involve a putative interaction (double-headed arrow) of the poly(A)-binding protein (PABP; gray ovals) with a yet unidentified factor X, which in turn interacts (directly or through other factors) with the 5′ leader (this putative interaction is shown by an open arrow). The eukaryotic translation initiation, elongation and termination factors are not shown. RNA elements are indicated as: curved box, ORF; thick lines, NTRs; $(A)_n$ and horizontal dashed line, poly(A) tail.

TOPO. The *Pac*I–*Xho*I fragment of 1F1-A_{50} was replaced by the similarly digested fragment of *fluc*-TOPO. B1-D1-A_{50} was designed by digestion of 1F1-A_{50} with *Dra*III and religation. To generate D1-F1-A_{50}, the *Pst*I–*Hin*dIII fragment of the RNA1 3′ NTR was inserted into pCR-BluntII-TOPO followed by digestion with *Sca*I and religation, producing 1–3′-7080–7481-TOPO. The *Pst*I–*Hin*dIII fragment of 1F1-A_{50} was replaced by the similarly digested fragment of 1–3′-7080–7481-TOPO. For creating F1-G1-A_{50}, 1F1-A_{50} was digested with *Apa*I, blunt-ended with T4 DNA polymerase (Fermentas) followed by digestion with *Hin*dIII, blunt-ending with Klenow enzyme (Promega) and religation.

To design 8C5′-A_{50} and 8C3′-A_{50}, the regions of 1F1-A_{50} upstream and downstream of the corresponding mutated site (nt 18–25 and 6361–6368, respectively) were PCR-amplified with two pairs of primers. For 8C5′-A_{50}, the primers 9+10 (upstream region) and 11+12 (downstream region) were used. The primers 13+14 (upstream part) and 15+16 (downstream part) were designed for 8C3′-A_{50} (Table 2). The resulting PCR products were inserted into pCR-BluntII-TOPO and accumulated in the *dam Escherichia coli* strain K12 ER2925 (New England Biolabs). The corresponding fragments, digested with *Aat*II/*Cla*I and *Cla*I/*Sph*I (for 8C5′-A_{50}) or *Sph*I/*Cla*I and *Cla*I/*Xho*I (for 8C3′-A_{50}), respectively, were ligated and introduced into 1F1-A_{50}. To create 8C5′/8C3′-A_{50}, the *Pst*I–*Xho*I fragment of 8C5′-A_{50} was replaced by the similarly digested fragment of 8C3′-A_{50}.

For generating 1F2-A_{50} (Fig. 5A), the *Pst*I–*Hin*dIII fragment of 1F1-A_{50} was replaced by the similarly digested fragment of 2F2-A_{50} (Karetnikov et al., 2006). 2F1-A_{50} (Fig. 5A) was obtained by replacing the *Pst*I–*Hin*dIII fragment of 2F2-A_{50} by the similarly digested fragment of 1F1-A_{50}. To produce 1FC-A_{50} and 2FC-A_{50} (Fig. 5A), the *Pst*I–*Hin*dIII fragment of 1F1-A_{50} or 2F2-A_{50}, respectively, was replaced by the similarly digested fragment of pETBlue-2 (Novagen) (nt 380–1740), PCR-amplified with primers 17 and 18 (Table 2).

For obtaining CF1-A_{50} (Fig. 2A), the construct pETΔ*Xba*I–*Nhe*I (Karetnikov and Lehto, 2007) was digested with *Eco*RV and *Hin*cII and religated, producing pETΔ*Eco*RV–*Hin*cII. The *Hin*dIII–*Not*I *fluc* fragment, PCR-amplified with primers 19 and 20, and *Not*I–*Pvu*II fragment of the RNA1 3′ NTR, PCR-amplified with primers 21 and 22, were ligated and cloned into pETΔ*Eco*RV–*Hin*cII. To add the poly$(A)_{50}$ tail, two complementary oligonucleotides, 23 and 24 (Table 2), were introduced by using the sites *Pvu*II and *Pml*I.

To produce 18S-B-A_{50}, 18S-C-A_{50} and 18S-B/C-A_{50}, the regions of 1F1-A_{50} upstream and downstream of the corresponding mutated or deleted sequence (nt 37–44, 50–58 and 37–58, respectively) were PCR-amplified with two pairs of primers. The upstream forward (primer 9) and downstream reverse (primer 12) primers (Table 2) were common for the three constructs. The other primers, containing the *Cla*I site, were used for obtaining 18S-B-A_{50} (primers 25 and 26), 18S-C-A_{50} (primers 27 and 28) and 18S-B/C-A_{50} (primers 25 and 28) (Table 2). The resulting PCR products were inserted into pCR-BluntII-TOPO and accumulated in the *dam E. coli* strain K12 ER2925. The corresponding fragments, digested with *Aat*II/*Cla*I and *Cla*I/*Sph*I, respectively, were ligated and introduced into 1F1-A_{50}.

For obtaining R1F1-A_{61} (Fig. 7), the *rluc* gene was PCR-amplified with primers 29 and 30, the RNA1 5′ NTR with primers 31 and 2, the *fluc* gene with primers 3 and 4 and the RNA1 3′ NTR with primers 5 and 22 (Table 2). The *rluc* gene was digested with *Xba*I, blunt-ended with Klenow enzyme and cloned into pETBlue-2, using the sites *Xba*I (blunt-ended) and *Nhe*I, resulting in the construct pET-*rluc*, harboring the T7 promoter. The other DNA fragments were digested with

Table 2
Oligonucleotides used in this study

Number[a]	Nucleotide sequence[b]	Restriction site encoded[c]	Nt position[d]
1	AGATCTtaatacgactcactatagggtttcaaaagctctttc	*Bgl*II	1–16
2	GTCGACtgtaaaatcaagaag	*Sal*I	52–66
3	GTCGACatgaggggatccgaag	*Sal*I	1–16
4	CTGCAGttacaatttggactttc	*Pst*I	1646–1662
5	CTGCAGcccaatagtgggttttatag	*Pst*I	6352–6371
6	AAGCTTgaaaggacatttcag	*Hin*dIII	7697–7711
7	AGCTT$(a)_{50}$A	*Hin*dIII, *Psc*I	NA[e]
8	CATGT$(t)_{50}$A	*Psc*I, *Hin*dIII	NA[e]
9	GACGTCtaagaaacc	*Aat*II	2617–2631
10	ATCGATaggaaagagcttttg	*Cla*I	4–18
11	ATCGATtttgccacctctttc	*Cla*I	24–39
12	GCATGCgagaatctg	*Sph*I	660–674
13	GCATGCcagagatcc	*Sph*I	669–683
14	ATCGATcactattgggctacc	*Cla*I	6347–6361
15	ATCGATataggtaaatagctag	*Cla*I	6367–6382
16	CTCGAGtagatgaattac	*Xho*I	6872–6889
17	CTGCAGctgtatacacgtgcaag	*Pst*I	380–396
18	AAGCTTgggagtcaggcaactatg	*Hin*dIII	1723–1740
19	AAGCTTatgaggggatccgaag	*Hin*dIII	1–16
20	GCGGCCGCttacaatttggactttc	*Not*I	1646–1662
21	GCGGCCGCcccaatagtgggttttatag	*Not*I	6352–6371
22	CAGCTGgaaaggacatttcag	*Pvu*II	7697–7711
23	CTG$(a)_{50}$CAC	*Pvu*II, *Pml*I	NA[e]
24	GAC$(t)_{50}$GTG	*Pml*I, *Pvu*II	NA[e]
25	ATCGATaagaggtggcaaaag	*Cla*I	23–37
26	ATCGATtatcttctcttcttg	*Cla*I	43–58
27	ATCGATagaagataaggagaaag	*Cla*I	35–51
28	ATCGATgattttacaGTCGAC	*Cla*I, *Sal*I	57–66
29	TCTAGAatgacttcgaaagtttatg	*Xba*I	1–19
30	GCTAGCttattgttcatttttg	*Nhe*I	920–936
31	GCTAGCtttcaaaagctctttc	*Nhe*I	1–16
32	CTAGAgaatacaagctacttgttctttttgcaCCC	*Xba*I, *Sma*I	1–27
33	GGGtgcaaaaagaacaagtagcttgtattcT	*Sma*I, *Xba*I	1–27

[a] Oligonucleotides 7, 8, 23, 24, 32 and 33 represent the complementary linkers encoding the poly$(A)_{50}$ tail (7, 8, 23, 24) and 27-nt fragment of the 5′ leader of *Xenopus laevis* β-globin mRNA (32, 33). Other oligonucleotides correspond to the PCR primers.
[b] Sequences of restriction sites, used for cloning, are in capitals. The sequence of the T7 promoter is underlined.
[c] Oligonucleotides 7, 8, 23, 24, 32 and 33 contain only partial sequences of the relevant restriction sites.
[d] Nucleotide (nt) positions are shown for BRV RNA1 (oligonucleotides 1, 2, 5, 6, 10, 11, 14–16, 21, 22, 25–28, 31), *fluc* cDNA (3, 4, 12, 13, 19, 20), *rluc* cDNA (29 and 30), *X. laevis* β-globin cDNA (32 and 33), pETBlue-2 (17 and 18) and pUC19 (9).
[e] Not applicable.

relevant restriction endonucleases and inserted into pET-*rluc*, producing R1F1. The poly$(A)_{61}$-containing *Sma*I–*Xba*I fragment of pET-A_{61} (Karetnikov and Lehto, 2007) was cloned into R1F1, digested with *Pvu*II and *Avr*II.

RCF1-A_{61} (Fig. 7) was produced as described for R1F1-A_{61}, except for introducing two complementary oligonucleotides, 32 and 33 (Table 2), representing the 27-nt fragment of the 5′ leader of *Xenopus laevis* β-globin mRNA, instead of the RNA1 5′ NTR, by using the sites *Xba*I and *Sma*I. For obtaining SR1F1-A_{61} (Fig. 7), the *Psc*I fragment of R1F1-A_{61} was replaced by the similarly digested fragment of SR2F2-A_{61} (Karetnikov and Lehto, 2007). The clone as-*fluc* has been described elsewhere (Karetnikov and Lehto, 2007).

In vitro transcription

DNA templates were linearized by *Pml*I (CF1-A_{50}), *Hin*dIII (1F1 and as-*fluc*), *Sda*I (dicistronic constructs) or *Psc*I (other constructs). RNAs were synthesized using the RiboMAX kit (Promega), as described previously (Karetnikov and Lehto, 2007; Karetnikov et al., 2006).

In vivo expression and protein analysis

Protoplasts from *N. benthamiana* plants were isolated, electroporated with RNA and incubated after electroporation, as in Karetnikov et al. (2006). Each experiment was repeated three times, with each electroporation performed in triplicate. Cell lysis, analysis of protein expression and estimation of mRNA translational efficiency and functional stability were carried out as described elsewhere (Karetnikov and Lehto, 2007).

Northern blotting

After 6 h incubation of electroporated protoplasts, total RNA was extracted with TRIzol (Invitrogen), and Northern blotting was performed by using the 600 nt digoxigenin-labeled antisense RNA probe as-*fluc*, as in Karetnikov and Lehto (2007).

Acknowledgments

We are grateful to Mika Keränen for help with computer analysis, Matti Karp and Pekka Virtanen for clones pPVc702 and pRL-SV40 and luminometer, Ari Hinkkanen for the Gene Pulser and Teemu Teeri for advices on protoplast work. This work was supported by Finnish Academy grants 40895 and 202652 and grants from the Finnish Cultural Foundation and the Kone Foundation.

References

Akbergenov, R.Zh., Zhanybekova, S.Sh., Kryldakov, R.V., Zhigailov, A., Polimbetova, N.S., Hohn, T., Iskakov, B.K., 2004. ARC-1, a sequence element complementary to an internal 18S rRNA segment, enhances translation efficiency in plants when present in the leader or intercistronic region of mRNAs. Nucleic Acids Res. 32, 239–247.

Algire, M.A., Lorsch, J.R., 2006. Where to begin? The mechanism of translation initiation codon selection in eukaryotes. Curr. Opin. Chem. Biol. 10, 480–486.

Baird, S.D., Turcotte, M., Korneluk, R.G., Holcik, M., 2006. Searching for IRES. RNA 12, 1755–1785.

Basso, J., Dallaire, P., Charest, P.J., Devantier, Y., Laliberté, J.-F., 1994. Evidence for an internal ribosome entry site within the 5′ non-translated region of *Turnip mosaic potyvirus* RNA. J. Gen. Virol. 74, 3157–3165.

Batten, J.S., Desvoyes, B., Yamamura, Y., Scholthof, K.-B.G., 2006. A translational enhancer element on the 3′-proximal end of the *Panicum mosaic virus* genome. FEBS Lett. 580, 2591–2597.

Bergamini, G., Preiss, T., Hentze, M.W., 2000. Picornavirus IRESs and the poly(A) tail jointly promote cap-independent translation in a mammalian cell-free system. RNA 6, 1781–1790.

Bradrick, S.S., Walters, R.W., Gromeier, M., 2006. The hepatitis C virus 3′-untranslated region or a poly(A) tract promote efficient translation subsequent to the initiation phase. Nucleic Acids Res. 34, 1293–1303.

Chappell, S.A., Edelman, G.M., Mauro, V.P., 2006. Ribosomal tethering and clustering as mechanisms for translation initiation. Proc. Natl. Acad. Sci. U. S. A. 103, 18077–18082.

Clyde, K., Kyle, J.L., Harris, E., 2006. Recent advances in deciphering viral and host determinants of dengue virus replication and pathogenesis. J. Virol. 80, 11418–11431.

Danthinne, X., Seurinck, J., Meulewaeter, F., Van Montagu, M., Cornelissen, M., 1993. The 3′ untranslated region of *Satellite tobacco necrosis virus* RNA stimulates translation in vitro. Mol. Cell. Biol. 13, 3340–3349.

Dinkova, T.D., Zepeda, H., Martínez-Salas, E., Martinez, L.M., Nieto-Sotelo, J., de Jiménes, E.S., 2005. Cap-independent translation of maize Hsp101. Plant J. 41, 722–731.

Dobrikova, E., Florez, P., Bradrick, S., Gromeier, M., 2003. Activity of a type 1 picornavirus internal ribosomal entry site is determined by sequences within the 3′ nontranslated region. Proc. Natl. Acad. Sci. U. S. A. 100, 15125–15130.

Dobrikova, E.Y., Grisham, R.N., Kaiser, C., Lin, J., Gromeier, M., 2006. Competitive translation efficiency at the picornavirus type 1 internal ribosome entry site facilitated by viral *cis* and *trans* factors. J. Virol. 80, 3310–3321.

Dorokhov, Yu.L., Skulachev, M.V., Ivanov, P.A., Zvereva, S.D., Tjulkina, L.G., Merits, A., Gleba, Yu.Y., Atabekov, J.G., 2002. Polypurine (A)-rich sequences promote cross-kingdom conservation of internal ribosome entry. Proc. Natl. Acad. Sci. U. S. A. 99, 5301–5306.

Doudna, J.A., Sarnow, P., 2007. Translation initiation by viral internal ribosome entry sites. In: Sonenberg, N., Hershey, J.W.B., Mathews, M.B. (Eds.), Translational Control in Biology and Medicine. Cold Spring Harbor Laboratory Press, Cold Spring Harbor, NY, pp. 129–153.

Dreher, T.W., Miller, W.A., 2006. Translational control in positive strand RNA plant viruses. Virology 344, 185–197.

Dresios, J., Chappell, S.A., Zhou, W., Mauro, V.P., 2006. An mRNA-rRNA base-pairing mechanism for translation initiation in eukaryotes. Nat. Struct. Mol. Biol. 13, 30–34.

Edgil, D., Harris, E., 2006. End-to-end communication in the modulation of translation by mammalian RNA viruses. Virus Res. 119, 43–51.

Elroy-Stein, O., Merrick, W.C., 2007. Translation initiation via cellular internal ribosome entry sites. In: Sonenberg, N., Hershey, J.W.B., Mathews, M.B. (Eds.), Translational Control in Biology and Medicine. Cold Spring Harbor Laboratory Press, Cold Spring Harbor, NY, pp. 155–172.

Fabian, M.R., White, K.A., 2004. 5′–3′ RNA–RNA interaction facilitates cap- and poly(A) tail-independent translation of *Tomato bushy stunt virus* mRNA. J. Biol. Chem. 279, 28862–28872.

Fabian, M.R., White, K.A., 2006. Analysis of a 3′-translation enhancer in a tombusvirus: a dynamic model for RNA–RNA interactions of mRNA termini. RNA 12, 1304–1314.

Florez, P.M., Sessions, O.M., Wagner, E.J., Gromeier, M., Garcia-Blanco, M.A., 2005. The polypyrimidine tract binding protein is required for efficient picornavirus gene expression and propagation. J. Virol. 79, 6172–6179.

Fraser, C.S., Doudna, J.A., 2007. Structural and mechanistic insights into hepatitis C viral translation initiation. Nat. Rev. Microbiol. 5, 29–38.

Gallie, D.R., 2001. Cap-independent translation conferred by the 5′ leader of *Tobacco etch virus* is eukaryotic initiation factor 4G dependent. J. Virol. 75, 12141–12152.

Gallie, D.R., 2007. Translational control in plants and chloroplasts. In: Sonenberg, N., Hershey, J.W.B., Mathews, M.B. (Eds.), Translational Control in Biology and Medicine. Cold Spring Harbor Laboratory Press, Cold Spring Harbor, NY, pp. 747–774.

Gallie, D.R., Tanguay, R.L., Leathers, V., 1995. The tobacco etch viral 5′ leader and poly(A) tail are functionally synergistic regulators of translation. Gene 165, 233–238.

Garlapati, S., Wang, C.C., 2004. Identification of a novel internal ribosome entry site in giardiavirus that extends to both sides of the initiation codon. J. Biol. Chem. 279, 3389–3397.

Garlapati, S., Wang, C.C., 2005. Structural elements in the 5′-untranslated region of giardiavirus transcript essential for internal ribosome entry site-mediated translation initiation. Eukaryotic Cell 4, 742–754.

Gazo, B.M., Murphy, P., Gatchel, J.R., Browning, K.S., 2004. A novel interaction of cap-binding protein complexes eukaryotic initiation factor (eIF) 4F and eIF(iso)4F with a region in the 3′-untranslated region of *Satellite tobacco necrosis virus*. J. Biol. Chem. 279, 13584–13592.

Griffiths, A., Coen, D.M., 2005. An unusual internal ribosome entry site in the herpes simplex virus thymidine kinase gene. Proc. Natl. Acad. Sci. U. S. A. 102, 9667–9672.

Guilley, H., Jonard, G., Kukla, B., Richards, K.E., 1979. Sequence of 1000 nucleotides at the 3′ end of *Tobacco mosaic virus* RNA. Nucleic Acids Res. 6, 1287–1308.

Gultyaev, A.P., van Batenburg, F.H.D., Pleij, C.W.A., 1995. The computer simulation of RNA folding pathways using a genetic algorithm. J. Mol. Biol. 250, 37–51.

Guo, L., Allen, E.M., Miller, W.A., 2001. Base-pairing between untranslated regions facilitates translation of uncapped, nonpolyadenylated viral RNA. Mol. Cell 7, 1103–1109.

Han, K., Byun, Y., 2003. PseudoViewer2: visualization of RNA pseudoknots of any type. Nucleic Acids Res. 31, 3432–3440.

Hentze, M.W., Gebauer, F., Preiss, T., 2007. *Cis*-regulatory sequences and *trans*-acting factors in translational control. In: Sonenberg, N., Hershey, J.W.B., Mathews, M.B. (Eds.), Translational Control in Biology and Medicine. Cold Spring Harbor Laboratory Press, Cold Spring Harbor, NY, pp. 269–295.

Herbreteau, C.H., Weill, L., Decimo, D., Prévôt, D., Darlix, J.-L., Sargueil, B., Ohlmann, T., 2005. HIV-2 genomic RNA contains a novel type of IRES located downstream of its initiation codon. Nat. Struct. Mol. Biol. 12, 1001–1007.

Hinnebusch, A.G., Dever, T.E., Asano, K., 2007. Mechanism of translation initiation in the yeast *Saccharomyces cerevisiae*. In: Sonenberg, N., Hershey, J.W.B., Mathews, M.B. (Eds.), Translational Control in Biology and Medicine. Cold Spring Harbor Laboratory Press, Cold Spring Harbor, NY, pp. 225–268.

Hu, M.C.-Y., Tranque, P., Edelman, G.M., Mauro, V.P., 1999. rRNA complementarity in the 5′ untranslated region of mRNA specifying the Gtx homeodomain protein: evidence that base-pairing to 18S rRNA affects translational efficiency. Proc. Natl. Acad. Sci. U. S. A. 96, 1339–1344.

Jaag, H.M., Kawchuk, L., Rohde, W., Fischer, R., Emans, N., Prüfer, D., 2003. An unusual internal ribosomal entry site of inverted symmetry directs expression of a Potato leafroll polerovirus replication-associated protein. Proc. Natl. Acad. Sci. U. S. A. 100, 8939–8944.

Jan, E., 2006. Divergent IRES elements in invertebrates. Virus Res. 119, 16–28.

Jang, S.K., 2006. Internal initiation: IRES elements of picornaviruses and hepatitis C virus. Virus Res. 119, 2–15.

Jünemann, C., Song, Y., Bassili, G., Goergen, D., Henke, J., Niepmann, M., 2007. Translation enhancement: picornavirus IRES elements can stimulate translation of upstream genes. J. Biol. Chem. 282, 132–141.

Kahvejian, A., Svitkin, Y.V., Sukarieh, R., M'Boutchou, M.-N., Sonenberg, N., 2005. Mammalian poly(A)-binding protein is a eukaryotic translation initiation factor, which acts via multiple mechanisms. Genes Dev. 19, 104–113.

Karetnikov, A., Lehto, K., 2007. The RNA2 5′ leader of *Blackcurrant reversion virus* mediates efficient *in vivo* translation through an internal ribosomal entry site mechanism. J. Gen. Virol. 88, 286–297.

Karetnikov, A., Keränen, M., Lehto, K., 2004. 3′ terminal sequences of *Blackcurrant reversion virus* (BRV) RNA2 are highly conserved in different virus isolates, and affect its translational efficiency. Acta Hort. (ISHS) 656, 109–114. http://www.actahort.org/books/656/656_16.htm.

Karetnikov, A., Keränen, M., Lehto, K., 2006. Role of the RNA2 3′ non-translated region of *Blackcurrant reversion nepovirus* in translational regulation. Virology 354, 178–191.

Kneller, E.L.P., Rakotondrafara, A.M., Miller, W.A., 2006. Cap-independent translation of plant viral RNAs. Virus Res. 119, 63–75.

Koh, D.C.-Y., Liu, D.X., Wong, S.-M., 2002. A six-nucleotide segment within the 3′ untranslated region of *Hibiscus chlorotic ringspot virus* plays an essential role in translational enhancement. J. Virol. 76, 1144–1153.

Koh, D.C.-Y., Wong, S.-M., Liu, D.X., 2003. Synergism of the 3′-untranslated region and an internal ribosome entry site differentially enhances the translation of a plant virus coat protein. J. Biol. Chem. 278, 20565–20573.

Komarova, A.V., Brocard, M., Kean, K.M., 2006. The case for mRNA 5′ and 3′ end cross talk during translation in a eukaryotic cell. Prog. Nucleic Acid Res. Mol. Biol. 81, 331–367.

Latvala-Kilby, S., Lehto, K., 1999. The complete nucleotide sequence of RNA2 of *Blackcurrant reversion nepovirus*. Virus Res. 65, 87–92.

Lehto, K., Lemmetty, A., Keränen, M., 2004. The long 3′ non-translated regions of *Blackcurrant reversion virus* RNAs are highly conserved between virus isolates representing different phenotypes and geographic origins. Arch. Virol. 149, 1867–1875.

Lemmetty, A., Latvala, S., Jones, A.T., Susi, P., McGavin, W.J., Lehto, K., 1997. Purification and properties of a new virus from blackcurrant, its affinities with nepoviruses, and its close association with blackcurrant reversion disease. Phytopathology 87, 404–413.

Levis, C., Astier-Manifacier, S., 1993. The 5′ untranslated region of PVY RNA, even located in an internal position, enables initiation of translation. Virus Genes 7, 367–379.

López de Quinto, S., Saiz, M., de la Morena, D., Sobrino, F., Martínez-Salas, E., 2002. IRES-driven translation is stimulated separately by the FMDV 3′-NCR and poly(A) sequences. Nucleic Acids Res. 30, 4398–4405.

Marin, C., Boronat, A., 1998. Nucleotide sequence of an *Arabidopsis* cDNA encoding a protein with similarity to mammalian polypyrimidine tract-binding protein (PTB) (accession no. AF076924) (PGR98–157). Plant Physiol. 118, 330.

Marintchev, A., Wagner, G., 2004. Translation initiation: structures, mechanisms and evolution. Q. Rev. Biophys. 37, 197–284.

Mauro, V.P., Edelman, G.M., 2002. The ribosome filter hypothesis. Proc. Natl. Acad. Sci. U. S. A. 99, 12031–12036.

Meulewaeter, F., Danthinne, X., Van Montagu, M., Cornelissen, M., 1998. 5′ and 3′-sequences of *Satellite tobacco necrosis virus* RNA promoting translation in tobacco. Plant J. 14, 169–176.

Meulewaeter, F., van Lipzig, R., Gultyaev, A.P., Pleij, C.W.A., van Damme, D., Cornelissen, M., van Eldik, G., 2004. Conservation of RNA structures enables TNV and BYDV 5′ and 3′ elements to cooperate synergistically in cap-independent translation. Nucleic Acids Res. 32, 1721–1730.

Miller, W.A., White, K.A., 2006. Long-distance RNA–RNA interactions in plant virus gene expression and replication. Annu. Rev. Phytopathol. 44, 447–467.

Mitchell, S.A., Spriggs, K.A., Bushell, M., Evans, J.R., Stoneley, M., Le Quesne, J.P., Spriggs, C., Willis, R.V., 2005. Identification of a motif that mediates polypyrimidine tract-binding protein-dependent internal ribosome entry. Genes Dev. 19, 1556–1571.

Mizumoto, H., Tatsuta, M., Kaido, M., Mise, K., Okuno, T., 2003. Cap-independent translational enhancement by the 3′ untranslated region of *Red clover necrotic mosaic virus* RNA1. J. Virol. 77, 12113–12121.

Mizumoto, H., Iwakawa, H., Kaido, M., Mise, K., Okuno, T., 2006. Cap-independent translation mechanism of *Red clover necrotic mosaic virus* RNA2 differs from that of RNA1 and is linked to RNA replication. J. Virol. 80, 3781–3791.

Mokrejš, M., Vopálenský, V., Kolenatý, O., Mašek, T., Feketová, Z., Sekyrová, P., Škaloudová, B., Kříž, V., Pospíšek, M., 2006. IRESite: the database of experimentally verified IRES structures. Nucleic Acids Res. 34, D125–D130 (www.iresite.org).

Niepel, M., Gallie, D.R., 1999. Identification and characterization of the functional elements within the *Tobacco etch virus* 5′ leader required for cap-independent translation. J. Virol. 73, 9080–9088.

Pacot-Hiriart, C., Latvala-Kilby, S., Lehto, K., 2001. Nucleotide sequence of *Blackcurrant reversion nepovirus* RNA1. Virus Res. 79, 145–152.

Pestova, T.V., Lorsch, J.R., Hellen, C.U.T., 2007. The mechanism of translation initiation in eukaryotes. In: Sonenberg, N., Hershey, J.W.B., Mathews, M.B. (Eds.), Translational Control in Biology and Medicine. Cold Spring Harbor Laboratory Press, Cold Spring Harbor, NY, pp. 87–128.

Qu, F., Morris, T.J., 2000. Cap-independent translational enhancement of *Turnip crinkle virus* genomic and subgenomic RNAs. J. Virol. 74, 1085–1093.

Rakotondrafara, A.M., Polacek, C., Harris, E., Miller, W.A., 2006. Oscillating kissing stem–loop interactions mediate 5′ scanning-dependent translation by a viral 3′-cap-independent translation element. RNA 12, 1893–1906.

Ray, S., Yumak, H., Domashevskiy, A., Khan, M.A., Gallie, D.R., Goss, D.J., 2006. *Tobacco etch virus* mRNA preferentially binds wheat germ eukaryotic initiation factor (eIF) 4G rather than eIFiso4G. J. Biol. Chem. 281, 35826–35834.

Scheets, K., Redinbaugh, M.G., 2006. Infectious cDNA transcripts of *Maize necrotic streak virus*: infectivity and translational characteristics. Virology 350, 171–183.

Serrano, P., Pulido, M.R., Saiz, M., Martínez-Salas, E., 2006. The 3′ end of the foot-and-mouth disease virus genome establishes two distinct long-range RNA–RNA interactions with the 5′ end region. J. Gen. Virol. 87, 3013–3022.

Shen, R., Miller, W.A., 2004. The 3′ untranslated region of *Tobacco necrosis virus* RNA contains a *Barley yellow dwarf virus*-like cap-independent translation element. J. Virol. 78, 4655–4664.

Shen, R., Miller, W.A., 2007. Structures required for poly(A) tail-independent translation overlap with, but are distinct from, cap-independent translation and RNA replication signals at the 3′ end of Tobacco necrosis virus RNA. Virology 358, 448–458.

Skulachev, M.V., Ivanov, P.A., Karpova, O.V., Korpela, T., Rodionova, N.P., Dorokhov, Yu.L., Atabekov, J.G., 1999. Internal initiation of translation directed by the 5′-untranslated region of the tobamovirus subgenomic RNA I_2. Virology 263, 139–154.

Song, Y., Tzima, E., Ochs, K., Bassili, G., Trusheim, H., Linder, M., Preissner, K.T., Niepmann, M., 2005. Evidence for an RNA chaperone function of polypyrimidine tract-binding protein in picornavirus translation. RNA 11, 1809–1824.

Song, Y., Friebe, P., Tzima, E., Jünemann, C., Bartenschlager, R., Niepmann, M., 2006. The hepatitis C virus RNA 3′-untranslated region strongly enhances translation directed by the internal ribosome entry site. J. Virol. 80, 11579–11588.

Susi, P., 2004. *Blackcurrant reversion virus*, a mite-transmitted nepovirus. Mol. Plant Pathol. 5, 167–173.

Svitkin, Y.V., Sonenberg, N., 2006. Translational control by the poly(A) binding protein: a check for mRNA integrity. Mol. Biol. 40, 611–619.

Svitkin, Y.V., Imataka, H., Khaleghpour, K., Kahvejian, A., Liebig, H.D., Sonenberg, N., 2001. Poly(A)-binding protein interaction with eIF4G stimulates picornavirus IRES-dependent translation. RNA 7, 1743–1752.

Terenin, I.M., Dmitriev, S.E., Andreev, D.E., Royall, E., Belsham, G.J., Roberts, L.O., Shatsky, I.N., 2005. A cross-kingdom internal ribosome entry site

reveals a simplified mode of internal ribosome entry. Mol. Cell. Biol. 25, 7879–7888.

Thivierge, K., Nicaise, V., Dufresne, P.J., Cotton, S., Laliberté, J.-F., Le Gall, O., Fortin, M.G., 2005. Plant virus RNAs. Coordinated recruitment of conserved host functions by (+) ssRNA viruses during early infection events. Plant Physiol. 138, 1822–1827.

Timmer, R.T., Benkowski, L.A., Schodin, D., Lax, S.R., Metz, A.M., Ravel, J.M., Browning, K.S., 1993. The 5′ and 3′ untranslated regions of *Satellite tobacco necrosis virus* RNA affect translational efficiency and dependence on a 5′ cap structure. J. Biol. Chem. 268, 9504–9510.

Tranque, P., Hu, M.C.-Y., Edelman, G.M., Mauro, V.P., 1998. rRNA complementarity within mRNAs: a possible basis for mRNA–ribosome interactions and translational control. Proc. Natl. Acad. Sci. U. S. A. 95, 12238–12243.

Vanderhaeghen, R., De Clercq, R., Karimi, M., Van Montagu, M., Hilson, P., Van Lijsebettens, M., 2006. Leader sequence of a plant ribosomal protein gene with complementarity to the 18S rRNA triggers in vitro cap-independent translation. FEBS Lett. 580, 2630–2636.

Wang, S., Miller, W.A., 1995. A sequence located 4.5 to 5 kilobases from the 5′ end of the *Barley yellow dwarf virus* (PAV) genome strongly stimulates translation of uncapped mRNA. J. Biol. Chem. 270, 13446–13452.

Wang, S., Browning, K.S., Miller, W.A., 1997. A viral sequence in the 3′ untranslated region mimics a 5′ cap in facilitating translation of uncapped mRNA. EMBO J. 16, 4107–4116.

Wu, B., White, K.A., 1999. A primary determinant of cap-independent translation is located in the 3′-proximal region of the *Tomato bushy stunt virus* genome. J. Virol. 73, 8982–8988.

Yang, D., Cheung, P., Sun, Y., Yuan, J., Zhang, H., Carthy, C.M., Anderson, D.R., Bohunek, L., Wilson, J.E., McManus, B.M., 2003. A Shine-Dalgarno-like sequence mediates in vitro ribosomal internal entry and subsequent scanning for translation initiation of coxsackievirus B3 RNA. Virology 305, 31–43.

Yilmaz, A., Bolinger, C., Boris-Lawrie, K., 2006. Retrovirus translation initiation: issues and hypotheses derived from study of HIV-1. Curr. HIV Res. 4, 131–139.

Zeenko, V., Gallie, D.R., 2005. Cap-independent translation of Tobacco etch virus is conferred by an RNA pseudoknot in the 5′-leader. J. Biol. Chem. 280, 26813–26824.

Zvereva, S.D., Ivanov, P.A., Skulachev, M.V., Klyushin, A.G., Dorokhov, Yu.L., Atabekov, J.G., 2004. Evidence for contribution of an internal ribosome entry site to intercellular transport of a tobamovirus. J. Gen. Virol. 85, 1739–1744.